P-ISSN: 2798-1134 | E-ISSN: 2797-3549 | DOI: 10.52562/injoes.2025.1596

Indonesian Journal of Earth Sciences

https://journal.moripublishing.com/index.php/injoes

| Research Article |

Structural Geomorphology and Tectonic Dynamism of the Lolodorf Segment, Nyong Complex, SW Cameroon

Messi Ottou Eric José[1,2]*, Etoundi Akoa Philémon Rémi[1], Ntieche Benjamin[3], Ntomba Sylvestre Martial[4], Evina Aboula Yannick Saturnin[2], Ndjigui Paul-Désiré[2]

[1]School of Geology and Mining Engineering, University of Ngaoundere, P.O. Box 115, Meiganga, Cameroon
[2]Department of Earth Sciences, Faculty of Science, University of Yaoundé I, P.O. Box: 812, Yaoundé, Cameroon
[3]Department of Biological Sciences, Geology Laboratory, Higher Teacher's Training School, University of Yaoundé I, P.O. Box: 47, Yaoundé, Cameroon
[4]Center for Geological and Mining Research, Institute for Geological and Mining Research, P.O. Box: 333, Garoua, Cameroon
**Corresponding author: ericjosemessiottou@gmail.com*

Received: 08 April 2025 / Accepted: 27 June 2025 / Published: 30 June 2025

Abstract: The study of the structural geomorphology and tectonic dynamism of the Lokoundjé and Nyong watersheds has made possible to discriminate the essential geological objects of the Lolodorf region (3°10'- 3°25'N, 10°40'- 10°55'E), in Southern Cameroon. This study has assessed the morphological and geological dynamism Lokoundjé and Nyong watersheds landscapes using both qualitative and quantitative data based on Digital Elevation Models (DEM) at 30 m resolution. Tectonic activities influence the topography of the land, which significantly affects the drainage system and geomorphological configuration of the area. Various tectonic indices were calculated to evaluate the evidence of tectonism. This includes hypsometric curve (HC) and hypsometric integral (Hi), relative tectonic uplift (U), longitudinal Profiles (PL), knick-points (kp), stream-length gradient index (SL-index) swath profile, Asymmetrie factor (AF), transverse topographic symmetric factor (TTSF), Basin shape (Bs) and Relative tectonic activity (Iat) cumulatively with linear, area, relief morphometric parameters, and hydrographic on 2 delineated basins of the study area. These parameters were used to elucidate the dynamism of the structural geomorphology of the Nyong Complex to best constrain the morphostructural environment of this region. Imbricated circular structures, which could correspond to the Ngovayang fault, are highlighted in the Mvoule, Mboulé, and Mvilé sub-basins for the first time. New faults are mapped, and the most important are the ductile corridors of the Lokoundjé, Ngovayang, and Mvilé with NE-SW direction, and finally, the faults of Mée, Mélangué Boulou, Elon, and Nyamfende with NW-SE direction. The topographical variations allowed us to subdivide the area of Lolodorf and its surroundings into three levels or domains and to highlight three main morphological units, namely the low, medium, and high units. Tectonic structure lithology and differential erosion control the nature of the geomorphology and hydrographic network of the study area. The combined classification of Relative Tectonic Activity Index (Iat) and morphometric parameters of 2 basins categorised all the zones into two different classes: Class 2-High (2.00) and Class 3-Moderate (2.17 - 2.33). The basins with tectonic activities have a consistent relationship with structural disturbances and basin geometry. The active tectonic zonation of part of the two basins, according to geomorphological indices and morphometric parameters, suggests a significant influence of tectonic activity in some parts of the two basins. It highlights the tectonic activity that occurred over time and its influence on the overall morphology extending to the entire southwest margin of Cameroon.

Keywords: Dynamism; Geomorphic indicators; Relative tectonic Activity index; Lolodorf Region; SW Cameroon

INTRODUCTION

The Lolodorf region (Fig. 1a-c) is located in the south of Cameroon and belongs to the Paleoproterozoic domain of the Nyong complex (NyC) bordering the Congo craton (Owona et al., 2011, 2012, 2013a; Messi Ottou et al., 2014a, b; Loose & Schenk, 2018; Ntomba et al., 2020). The lithology highlights the Nyong, Oubanguide, and Sedimentary Complexe. The NyC consists of orthogneisses, charnockites, mylonites, amphibolites, métasyénites, metagranodiorites, and eclogites (Nsangou Ngapna et al., 2013; Loose & Schenk, 2018). The Oubanguide Complex (OuC) consists of paragneisses, micaschists, chloritoschists, and quartzites. And the sedimentary complex consists of conglomerates, coarse sandstones, silts, clays, limestones, ferruginous sands, and enriched marls (Nsangou Ngapna et al., 2013). The major known structural feature is the fault zone of the Lokoundjé with NE-SW direction (Maurizot et al., 1986).

The action of the humid equatorial climate on the Proterozoic basement allowed the development of a relief with altitudes ranging from 190 m to 1061 m covered with a very important pedo-vegetal cover. The scarcity of outcrops due to severe weathering and vegetation makes traditional mapping surveys in the field quite difficult. A similar approach has been used previously in different regions (Shukla et al., 2014) to determine the relative tectonic activity index (Iat) using morphometric and geomorphic index parameters as a decisive tool among many others. They have shown that the evolution of landforms is influenced by a variety of elements, including lithology, tectonic activity, and climate. In particular, the geodynamic conditions brought about by tectonic plate motions regulate the lithology and topography, where tectonic activity can have a direct or indirect regulatory effect (Bull, 2007). Nevertheless, selecting suitable indices is still difficult, considering deformation rates, tectonic source types, and all other variables that can influence geomorphic processes (Figueiredo et al., 2019). In this study, we incorporated linear, areal, and relief parameters along with geomorphic indices, which have been used to determine the relative tectonic activity of the basin. It also limits the connections between tectonics, the Lolodorf region's lithology, and the landscape's evolution.

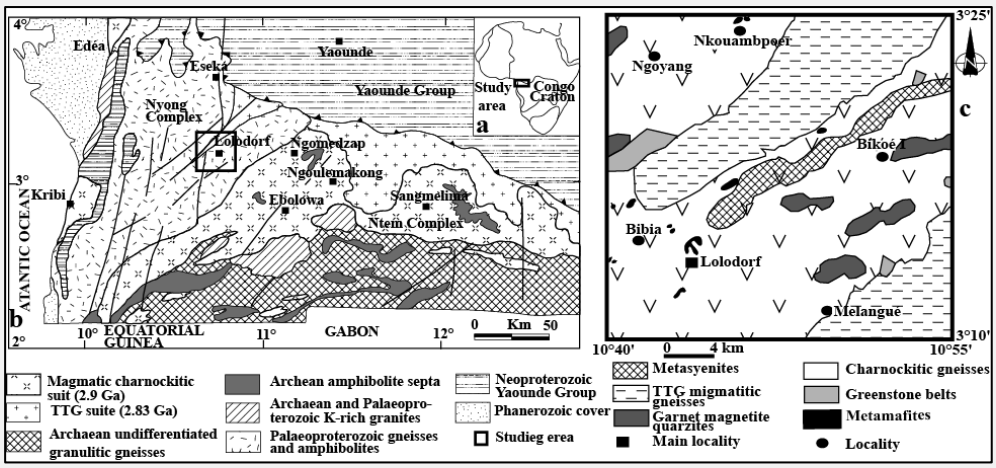

Figure 1. Location and geology of the Lolodorf region. a) - Map of Cameroon in central Africa; b) - Simplified geological map of southwestern Cameroon (modified from Maurizot et al., 1986, c) - Schematic map of the studied area modified after (Lerouge et al., 2006; Loose & Schenk, 2018; Bouyo et al., 2019; Messi Ottou et al., 2022).

GEOLOGICAL & GEOMORPHOLOGICAL SETTINGS

Geological settings

The study area lies within Lolodorf along a stretch of National Yaoundé-Kribi. This stretch of Lolodorf and its surroundings (3°10' - 3°25'N, 10°40' - 10°55'E; Fig. 1b,c) lies within the lesser belongs to the central part of the Eburnean belt of SW Cameroon called NyC (Owona et al., 2011, 2012, 2013a,b; Messi Ottou et al., 2014a; Ntomba et al., 2016; Loose & Schenk, 2018). The lithology of the NyC is highly variable and is composed of gneisses, tonalite-trondhjemite-granodiorite (TTG), anorthosites, charnockites, migmatites, eclogites, metagabbros, quartzites, banded ironstone formations (BIF), potassium granitoids, metasyenites, pyroxenites, and metagranodiorites (Tchameni et al., 2000; Shang et al., 2004; Lerouge et al., 2006; Pouclet et al., 2007; Owona et al., 2011, 2012; Abeng et al., 2012; Nsangou Ngapna et al., 2013; Loose & Schenk, 2018), hosted in metamorphic formations. The study area includes to the northwest garnet magnetite quarzites, charnockitic gneisses, greestone belts, and granulites. The central part consists of garnet magnetite quarzites, charnockitic gneisses, greestone belts, TTG migmatitic gneisses, metasyenites, and granulites. The southwestern part of the study area mainly comprises TTG migmatitic gneisses, greestone belts, and granulites (Fig. 1c; Lerouge et al., 2006; Loose & Schenk, 2018; Bouyo et al., 2019; Messi Ottou et al., 2022). Vicat et al. (1998) studied the basal rocks of the Lower Archean Greenstone Belt of Lolodorf-Ngomezap and highlighted ortho-amphibolites from gabbros and dolerites dated around 3.2 Ga. They were affected by a polyphaser deformation marked by the emplacement of the Nyong aquifer transported eastwards on the Congo craton and dissected by NW-SE-orientated blastomylonitic shear corridors (Maurizot et al., 1986; Nédélec et al., 1993; Feybesse et al., 1998; Pénaye et al., 2004; Lerouge et al,. 2006; Owona et al., 2011).

Geomorphological settings

From the geomorphological point of view, the large-scale landscapes of SW Cameroon in the NyC are characterised by the coastal plain and the southern Cameroon plateau (Ségalen, 1967). The coastal plain is made up of three successive levels towards the southern Cameroonian plateau with an average altitude of 750 m (Njiké Ngaha, 1984): the first altitude stage 0 - 150 m extends over nearly 100 km from the coast. It is made up of gently sloping hills (< 3%) with spreading peaks. The transition to the upper level is gradual; the second level has altitudes that oscillate between 151 m and 250 m and extend over 50 km. It has flat-topped hills with low slopes (about 5%). The monotony of the relief is broken by the upper altitude unit; the third level has altitudes between 251 m and 350 m; it is made of hills with convex peaks and slopes of the order of 6 to 10%. It extends over approximately 50 km. The contact of this level with the southern Cameroonian plateau is marked by a difference in level exceeding 200 m (Ndjigui et al., 2009).

The South Cameroon plateau is a geomorphological entity attached to the African surface I (Ségalen, 1967), which extends over 600 km from west to east to beyond Yokadouma. Its average altitude is 700 m. It is around 800 m in the north, 600 m in the center, rises to 750 m around Yaoundé, and decreases in stages towards the south. The presence of these plateaus suggests that the southern Cameroonian plateau would have been affected by tectonic movements.

MATERIALS & METHODS

The geomorphometric indices taken from the 30 m pressure digital elevation model (DEM) for the geomorphological approach (Bull & McFadden, 1977; Lifton & Chase, 1992; Keller & Pinter, 1996; Ramírez-Herrera, 1998; Pérez-Peña et al., 2009) were correlated with the available geological (1/500,000), hydrogeological (1/500,000), and topographical (1/50,000) maps. Furthermore, several field photos employed to determine the tectonic and confluent nature of knick-points (kp) in the longitudinal profiles of the rivers (Keller & Pinter, 2002; Kirby & Whipple, 2012; Koukouvelas et al., 2020) and to address uncertainties arising from the correlation between the 30 m pressure DEM and the available small-scale maps (Koukouvelas et al., 2018).

Additionally, more morphometric indices added. Using the qualitative geomorphology approach, the relief variations and their relationships with orographic and lithostructural variations characterized, with a focus on regional features like scarps and faults, by using geological and topographic maps as slope shading of the hydrographic network from ArcGIS software (GIS-type software). They connected with NASA-provided SRTM-1 (Shuttle Radar Topographic Mission) photos in order to overcome the accuracy constraints of automatic hydrographic network extraction. Lithostructural controls, roughness and incision highlighted on the basis of the analysis of topographic cross-sectional profiles, 3D block diagrams produced by Surfer 13. By creating the directional rosettes, we were able to analyse the primary flow directions of the rivers in the Geoplot application. The morphological and tectonic controls of landform evolvement are often expressed by the slopes that are shown. Topographic contrast, mountain escarpment front, slope value, and differences in incision and roughness, are suitable tools to differentiate different morphological units.

Quantitative analysis has been applied by using geomorphic indices pertained in order to understand how the landform in the Lolodorf region has adjusted to deformation. The main geomorphic indices computed are Normalized longitudinal profiles of rivers (LPs) and knic-points (Kp), Stream Length index (SL-index), Relative tectonic uplift (U), Asymmetric factor (AF), Transverse topographic symmetric factor (T), Basin shape (BS), Hypometric integral (Hi), and relative tectonic activity (Iat). Table 1 summarizes the formulas, equations and parameters used for their calculation, the threshold values interpretation and the main classes of tectonic activity.

The longitudinal profiles (LPs) and associate knick-points (Kp), Stream length-gradient index (SL-index) and relative uplift (U), are very efficient to detect patterns of differential tectonic uplift (Wobus et al., 2006, Kirby & Whipple, 2012). LPs through their channel gradient variations, geometry and knick-points, express the interaction between fluvial incision, lithological patterns, active tectonic processes, sea-level and climate changes (Willgoose & Hancock, 1998; Keller &Pinter, 2002; Huang & Niemann, 2006; Mvondo Owono et al., 2016; Ali & Ikbal, 2020). Convex longitudinal profiles are characteristics of young river or old rivers reactivated by fault or affected by uplift while concave one are characteristics of old rivers, in equilibrium state. Kp show disturbances of the river equilibrium state that led to change in the base level of tectonic or eustatic origin, changes in rock erodibility, changes in the local slope caused by active tectonics (faulting), or changes in the load carried by the river (Hack, 1973; Burbank & Anderson, 2001; Keller & Pinter, 2002; Kirby & Whipple, 2012). Kp were meticulously documented

along with their elevation above sea level, gradient, lithology, confluence, or faults, as well as the distances to the source and outlet.

Table 1. Geomorphic indices used for landscape analysis: formula and equation for their calculation and threshold values interpretation

Geomorphic indices	Formula or equations and parameters	Threshold values interpretation	References
Normalized longitudinal profiles of rivers	y-y0 = (y1-y0/(x1-x0) + (x-x0) y: elevation in normal range; x: distance in logarithmic scale $A_N = A_m + (((A_H - A_L)/(LogL_m - LogL_M))*(Log\ L_i - LogL_M)$ A_N :equilibrium normalised altitude value A_H and A_L: Highest and lowest altitude L_M and L_m: Maximum and minimum length L_i: length value calculated for each considerate point in relation with the upstream	• Concave longitudinal profiles are characteristic of old rivers, in equilibrium state • Convex longitudinal profiles are characteristics of young rivers or old rivers reactivated by fault of affected by uplift	(Mvondo Owono et al., 2011, 2016)
Stream length index (SL-inex)	SL-index = (ΔH/ΔL)*L ΔH: difference elevation between the ends of considered reach; ΔL: length of the reach; L: distance between the measure reach and the drainage divide	Very high or very low SL index value reveal tectonic distortions if there is no correlation with the lithological factors	(Hack, 1973)
Relative uplift (U)	U = hm + (1-Hi) hm: mean elevation for 50% of area; Hi: integral hypsometry	• U ≥ 1: very high uplift: class 1; • 0.7 ≤ U < 1: high uplift: class 2; • U < 0.7: low uplift: class 3	(Sinha-Roy, 2002)
Asymmetry factor (AF)	AF = | 50-(Ar/At)*100 | A_r: area of the basin to the right of main channel facing downstream A_t: Total area of the basin	• AF ≥ 15: very high tilting: class 1 • 10 ≤ AF < 15: high tilting: class 2 • 5 ≤ AF < 10: moderate tilting: class 3 • AF < 5: no or low tilting: class 4	(Hare & Gardner, 1985; Keller & Pinter, 2002)
Transverse topographic symmetric factor (T)	T = Da/Dd D_a: distance between symmetry axis of the basin and river D_d: distance between axis of the basin and the border of the same basin	• T ≥ 0.4: High asymmetry: class 1 • 0.2 < T < 0.4: moderate asymmetry: class 2 • T ≤ 0.2: low asymmetry: class 3	(Cox, 1994; El Hamdouni et al., 2008)
Basin shape (BS)	Bs = Bl/Bw Bl: basin length form head point to mouth Bw: width of the basin	• BS > 4: elongated basin: class 1 • 3 ≤ BS ≤ 4: semi-elongated basin: class 2 • 3 BS < 3: circular basin: class 3	(Ramirez-Herrera, 1998; El Hamdouni et al., 2008)
Hypsometric integral (Hi)	$Hi = (H_{avg} - H_{min})/(H_{max} - H_{min})$ H_{avg}, H_{max} and H_{min}: average, maximum and minimum elevation	• Hi >0.4: younger stage of basin development, most of the topography is high relative to the mean: class 1 • 0.3 ≤ Hi < 0.39: mature basins, extensive and long-term erosion, associated with dissected drainage basins: class 2 • Hi < 0.3: older basins, such as peneplains: class 3	(Keller & Pinter, 2002; Anand et al., 2019)

To distinguish Kp connected to faults from those connected to lithological boundaries or river confluences, cross sections with longitudinal profiles were conducted. SL-index is used as a quantitative parameter developed by Hack (1973) and Keller & Pinter (2002) in order to evaluate tectonic effects of river forms and drainage patterns. It computed for each 1 km of main river length in order to determine local uplift and their incipient local response to regional tectonic events and to reinforce Kp identification.

U seem to be efficient in distinguishing zones affected by different uplift rates (Kirby & Whipple, 2012). Uplift (U) values the elevation increase in excess of denudation during the formation of the actual drainage system (Mathew et al., 2016; Nsangou Ngapna et al., 2020; Sinha-Roy, 2002). It is not the absolute magnitude of tectonic uplift. It reveals spatial variations of uplift magnitude in the sub-catchment.

To characterize the tilting of a basin due to an uplift or the replay of a fault, two main geomorphic parameters calculated, the drainage basin asymmetry (AF) and the Transverse Topographic Symmetry Factor (T; Alipoor et al., 2011; Eynoddin et al., 2017). AF is observed when the basin is tectonically tilted perpendicular to its longitudinal trend, and the stream shifts its course (Hare & Gardner, 1985; Keller & Pinter, 2002; Taloor et al., 2021; Thakkar et al., 2021). This indices is very suitable for assessing the magnitude of the tilting at scale of a drainage basin over a relatively large area. Streams formed under the influence of active tectonics can reflect the direction of deformation. As for TTSF, it evaluates the amount of asymmetry of a stream within a catchment and the variation of this asymmetry in different segments of the valley (Mathew, 2016). TTSF gives information about the tilt direction and helps understand the level of tectonic activity in the area (Cox, 1994; Eynoddin et al., 2017). For a perfectly symmetric basin T = 0, as the symmetry decreases, T approaches the value of 1 assuming that shift of stream channels is an indication of possible surface tilting resulting in variation of slope polarity and the influence of bedrock on stream migration is negligible. Bs indicated the shape of the basin and its relation with the relative tectonics. Elongated shape basins indicate active tectonics, while circular shape constitutes less active tectonics (Bull & Mc Fadden, 1977; El Hamdouni et al., 2008). The elongated shapes are transformed into circular basins, as tectonic activity reduces with the time and continued topographic evolution (Bull & McFadden, 1977).

The basin geomorphological development period, as well as the relief's dissection and evolution, are revealed by the HC's shape. Young, active watersheds with low erosion effects or old basins revitalised by tectonics are indicated by convex curves; mature basins with moderate erosion processes are indicated by S-shaped curves; and old (peneplain) watersheds with strong erosion processes are indicated by concave curves (Harlin, 1978; Mayer, 1990). Hi shows the elevation of a certain area or relief, which represents an uneroded area under the hypsometric curve, and displays intricate relationships between erosion and tectonics connected to uplift rates. Watersheds in the young stage are represented by convex curves with high Hi values, those in the mature stage by concavo-convex or straight curves, and those in the old stage by concave curves with low Hi values (Strahler, 1952; Mayer, 1990; Keller & Pinter, 2002; Xue et al., 2017; Sheikh Mohideen, 2021; Aju et al., 2022).

El Hamdouni et al. (2008), Alipoor et al. (2011), Mahmood & Gloaguen (2012) and Anand & Pradhan (2019) all use Iat to characterise the geographical distribution of relative active tectonics in specific regions. The geomorphological indices and surface morphometric characteristics were divided into various classes in this study, and the average values of these classes were taken into account when evaluating the Iat. El Hamdouni et al. (2008) and Anand & Pradhan (2019) classified the values into four classes according to the relative tectonic activity level: class 1 (1.0 - 1.5), class 2 (1.5 - 2.0), class 3 (2.0 - 2.5), and class 4 (> 2.5). These classes represent very high, high, moderate, and low relative tectonic activity, respectively.

RESULTS

Relief Parameters

Geomorphology units

The relief of Lolodorf and surroundings is a peneplain with elliptic, polygonal, and sub-round shapes illustrated by the topographic contours. It consists of semi-orange hills resulting from an alternation of a few valleys and circular hillocks with relatively sharp summits separated by shallow passes (less than 20 m vertical drop). The topography illustrates convex and concave circular peaks (Fig. 2a,b) that make the landscape monotonous in places.

The topographic variations allowing the staging and spatial arrangement of the relief allowed us to subdivide the Lolodorf area and its surroundings into three bearing levels or domains (Fig. 3 and Table 2). The first landing (I) or NW domain occupies the NW with altitudes ranging between 190 and 1100 m; its boundary with the landing (II) or central area is a NE-SW escarpment coupled with a deep valley that suggests a major tectonic action. It could be linked to a continental uplift NE-SW. The Ngovayang Range is an elliptical hill whose extension axis is NE-SW and that of compression is NW-SE. The 3D map and DEM show a plateau summit marked by vertices and valleys also orientated NE-SW (Figs. 2a-c & 3). The second level (II), or central area, covers the central part at average altitudes of 480 m, with some peaks between 600 and 834 m. This area constitutes the Lolodorf multi-kilometer collapse ditch,

orientated SW-NE. It could correspond to a continental slump in the same direction. This bearing is the Lolodorf depression, dominated by asymmetric isolated hills in the center and narrowed NE (Figs. 2a-c, 3). As for the landing (III) or SE area, which covers the NNE and a part of the south of the region whose altitudes vary between 400 and 940 m, representing the hills of Mvengué that cover the SE part, it is a high plateau dissected by deep valleys that individualise NE-SW to E-W-orientated Mvengué hills (Figs. 2a-c, 3).

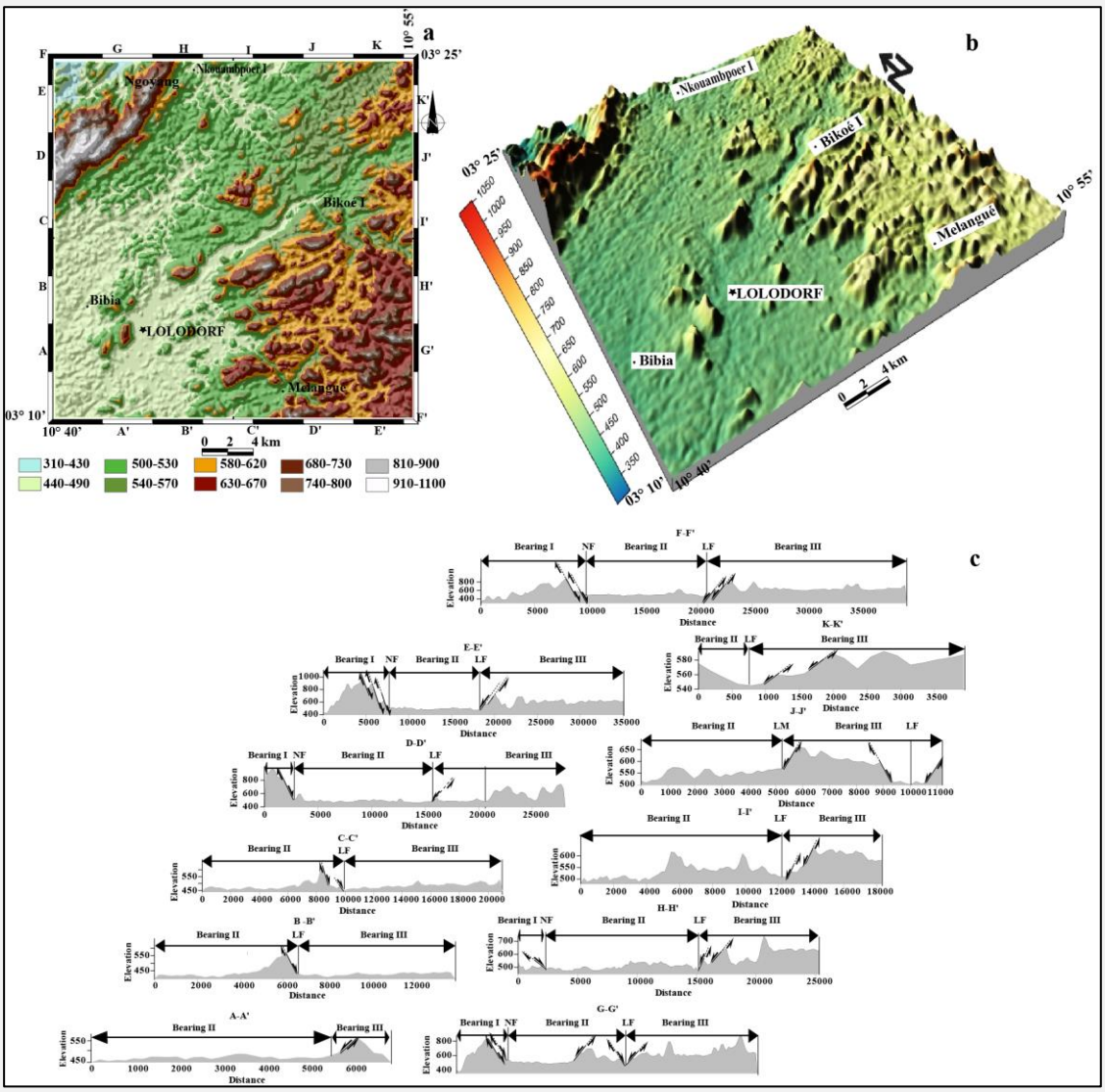

Figure 2. a) - Map of morphological units of the Lolodorf region and its surroundings made from the image SRTM_u03_p186r058.tif. at 1/50000; b) - Block diagram of the Lolodorf region and its surroundings made from (image SRTM_u03_p186r058.tif at 1/50000) and c) - NW-SE serial topographic profiles perpendicular to the maximum elongation of bearings I, II and III. Note the normal faults responsible for the collapse ditch and the dullness of the reliefs.

In the Lolodorf region and its surroundings we have identified three main geomorphological units (Fig. 2a): (a) the base unit (altitudes below 570 m) has a high concentration in the North, Centre, and South; (b) the average unit (570 < altitude < 800 m) is mainly located in the SE with a few islands at SW, Center, NE, and a hill at the NW; (c) the high unit (altitude > 800 m) is generally located in the NW with a few islands in the Center, NE, East, and SE.

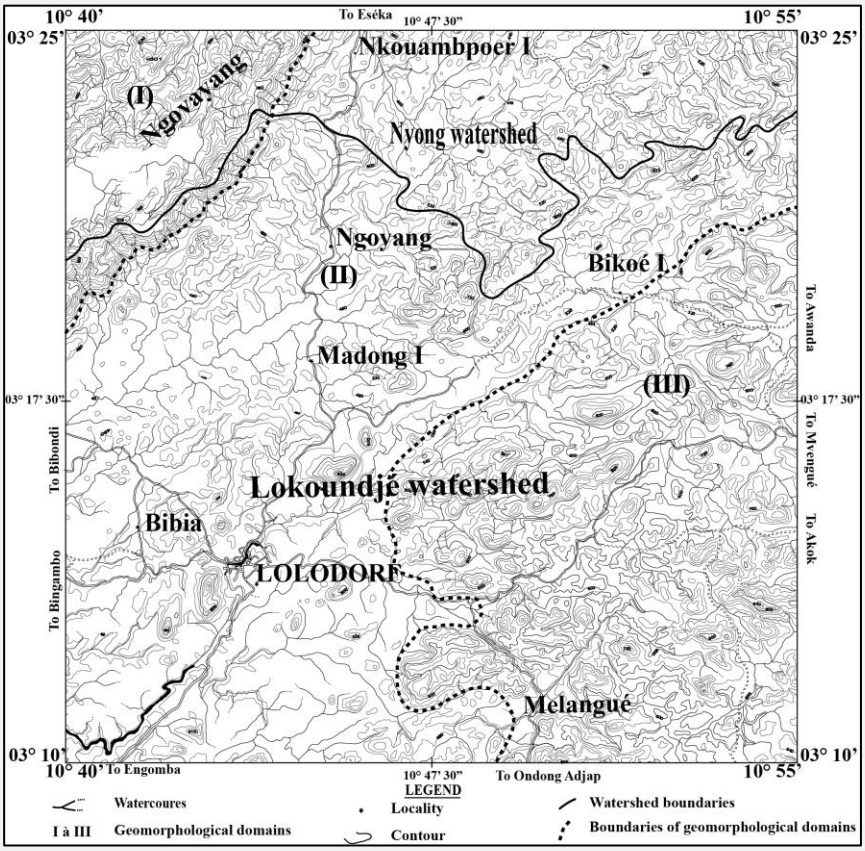

Figure 3. Topographic map of the Lolodorf region (Extracted from the Edea 2A forest map, NA - 32 - XXIII - 2a leaf, Edea 2B, NA - 32 - XXIII leaf 2b, Edea 2C, NA - 32 - XXIII - 2c leaf and Edéa 2D, sheet NA-32-XXIII-2d at 1/50000) showing: - NW unit (I), - central unit (II) et - SE unit (III).

Table 2. Relief parameters of the Lolodorf region

		Unit I	Unit II	Unit III
Hill	Altitude	190 m < Z < 1100 m	432 m < Z < 940 m	190 m < Z < 834 m
	Terracing	High	Valley NE-SW	High
	Slope	Steep (25° - 40°)	Slow (0° - 15°)	Slight to middle (15° - 35°)
	Typology	Ngovayang chain Top and small valley NE-SW	Lolodorf depression Dissymmetrical and isolated hill at center in NE	Collines de Mvengué NE-SW hill individual by valley
Differential erosion	Roughness	High	Slow	High
	Incision	Avarage in valley with escarpment	Average	High at escarpment
	Erosion	High with bulled top	Slow into depression	High with bulled top

Slope

On the basis of the stiffness or not of the slope, three zones were recorded (Fig. 4a-e). The average slope in the bearing (I) has values between 15 and 30%, indicating the presence of many escarpments, of which the brightest (> 45%) marks the limit with the bearing (II), whose average slope is less than 10%. Only isolated hills in the center of depression have a slope exceeding 30%. Within the plateau (III°), the three orographic levels corresponding to the relief steepness on low (< 10%), medium

(10-20%), and steep (> 20%) slopes are represented. The alignment and spatial arrangement of steep slopes and low slope escarpments suggest both tectonic control and variable erosion resistance.

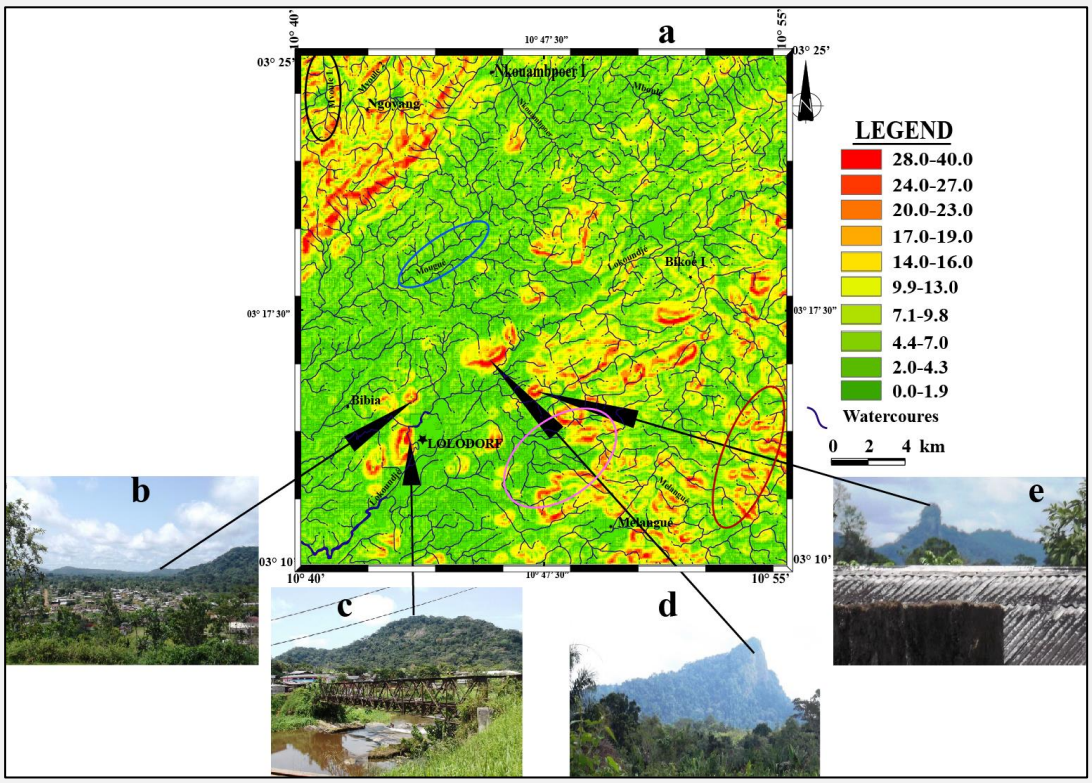

Figure 4. a) - Map of the slopes of the Lolodorf region and its surroundings extracted automatically from the SRTM image; b-e) - Tops of some hills illustrating their slopes.

Hydrographic Parameters

Typology

The Lolodorf region watershed is part of the Lokoundjé and Nyong watersheds and is globally dendritic (Fig. 5a). However, it presents angular, radial, parallel, and circumvented trends. Its main parameters are recorded in Table 3.

The Lokoundjé watershed represents 4/5 of the river system in the study area. It can be subdivided into three (03) subwatersheds: the Lokoundjé, the Mougué, and the Melangué, whose waters flow globally from NE to SW as the regional collector the "Lokoundjé". The springs that feed them flow in all directions, like the water courses of orders 1 and 2. The flows of these tributaries and all rivers of higher orders become uniform according to the preferred direction NE-SW and secondarily more or less in the N-S, NW-SE, and E-W directions (Fig. 5a). The Nyong watershed occupies the remaining 1/5 of the river system of the study area. It can also be subdivided into three (03) subwatersheds: Mvoulé, Mboulé, and Mvilé, whose waters flow globally from south to north to be poured into the Nyong River, which flows from east to west. Its tributaries and springs (water courses of orders 1 and 2) flow globally in the E-W, NE-SW and N-S directions. The flows of these tributaries, higher-order rivers, become more or less uniform along the NW-SE and N-S directions (Fig. 5a).

The configuration of the hydrographic network and flows in NE-SW, N-S, NW-SE, and E-W directions in the Lokoundjé and Nyong watersheds suggests their parallelism with the alignment of escarpments and valleys and the distribution of the slopes mentioned above. The dendritic nature of this network would indicate its development on an impervious basement. His parallel and angular tendencies testify to his tectonic control. The deepness of the valleys that shelter this hydrographic network seems to indicate the major role of the runoff waters in their degradation.

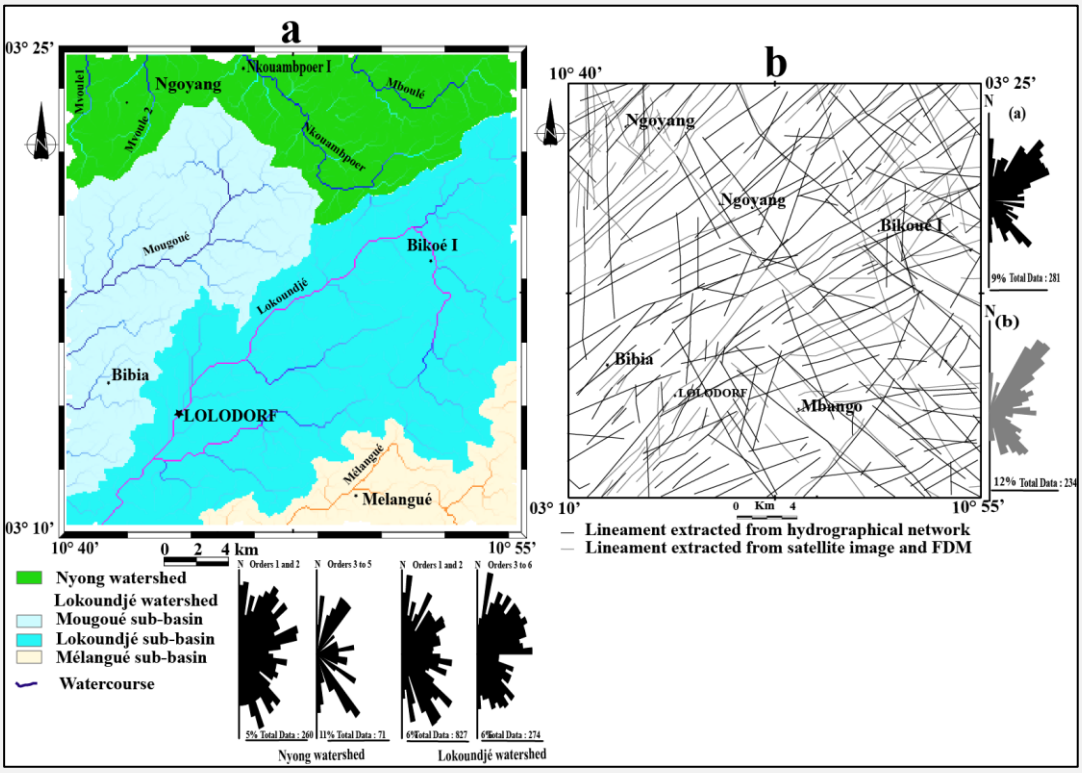

Figure 5. a) Watershed distribution map associating the rosettes of the directions of the watercourses of the Lolodorf region and its surroundings; b) Synthetic linear map of the lineaments associated with rosettes representing the frequencies of the directions.

Table 3. Hydrographic parameters of the main collectors of Lolodorf region

Watersheds		Lokoundjé	Nyong
Sub-catchments		Lokoundjé, Mougué et Melangué	Mvoulé 1, Mvoulé 2, Nkouambpoer et Mboulé
Typology		Dendritic to paralled, angular, radial and contorted	Dendritic to paralled, angular
Flow sense and directions	Important	NE →SW	E →W
	Secondary	E →W and N →S	NE →SW and N →S
Hypsometry		Peneplain and mature basin (Hi=0.06; 0.25; 0.35)	Mature basin (Hi=0.35)
Equilibrium profile		In stair step with rises of breaks of slopes (kp)	In stair step with rises of breaks of slopes (kp)

Hydrographical anomaly and lineament

The method of Deffontaines & Chorowicz (1991) allowed us to interpret the structural elements that caused the profound changes in the hydrographic pattern. The structural directions NE-SW and SE-NW are well marked by the hydrographic network. The streams lineaments do not follow a uniform direction, and these are guided by the morphostructures of the lands crossed, giving irregular rectilinearities (brown ellipse), pinches (blue ellipse), curvatures (pink ellipse), directional changes (pink ellipse), and asymmetries of confluences (black ellipse) (Fig. 4). E-W and N-S directions are less visible. The directions of the great tectonic lineaments of Cameroon (Cameroon Volcanic Line (CVL) N025 to N040, Sanaga and that of Adamaoua N065 to N070), the sub-regional ("Cameroon-Gabon" N005 to N015) and those of the Gulf of Guinea (N105 to N145) (Dumont, 1986; Thierry et al., 2006) are well marked by their layout and thus influence the hydrographic system of the region (Fig. 5a).

The typological analysis of the linear map (Fig. 5b) from the DEM, satellite images, and the topographic map shows lineaments equivalent to foliation trajectories and faults parallel to escarpments, ridge lines, valleys, and some portions of the river system (Figs. 2a,b, 4, 5a) indicated an unequal distribution of the tectonic fracture network. The lineaments define different sectors: a North-West sector, a Central sector, and a South-East sector; equivalent to levels (I), (II), and (III). The bearing (I) is poorly traversed by a few lineaments with NE-SW and N-S directions. The bearing (II) is incised by NE-SW linear directional, two of which constitute its NW and SE boundaries. They are orientated NE-SW, ENE-WSW, NW-SE and E-W in the landing (III). These correspondences suggest the existence of a link between these lineaments and the marks of the relief and the hydrographic network. The predominantly parallel orientations of the lineaments suggest their geological origin.

Geomorphic indices

Geomorphic indicators were determined to analyse topography, drainage networks and the role of relative active tectonics in the deformational process (El Hamdouni et al., 2008; Topal et al., 2016). The geomorphological indices were determined for the 2 basins that are part of the Nyong basin (Mvoulé 1, Mvoulé 2, Nkouambpoer, and Mboulé) and the Lokoundjé (Lokoundjé, Mougué, and Melangué Table 3). The parameters of the geomorphological indices were averaged with the linear, areal, and relief parameters to determine the Iat.

Hypsometric curve (HC) and integral (Hi)

The hypsometric curve (HC) produced in the Nyong basin (Nkoumbpoer river) is convex and those of the Lokoundjé basin in the Mougoué river have a concave shape. While the Lokoundjé and Mélangué combine concave shapes and are convex (Fig. 6a). The integral hypsometries (Hi) of Nyong (Nkouampoer), Mougoué, Lokoundjé, and Mélangué are respectively around 0.35, 0.06, 0.25, and 0.35. But in this study, we used the classification of Anand & Pradhan (2019), which cuts out new intervals of Hi and integrates new interpretations but still retains three classes as in the classification of Ali & Ikbal (2020). The Hi of Nyong and Mélangué have a value of 0.35, corresponding to class 2, which reflects mature basins linked to extensive erosion over time and to dissected drainage basins; on the other hand, the Hi of Mougoué and Lokoundjé are less than 0.30, correlable to class 3, which materialises the oldest watersheds corresponding to the peneplains (Fig. 6b). In the study area, class 1 (Hi ≥ 0.4), which corresponds to the youngest basins correlable to above-average topography, is not represented.

Relative tectonic uplift (U)

Mathew (2016) distinguished three classes to characterise U. In class 1 ($U \geq 1$), subsidence is very low, while in class 2 ($0.90 \leq U < 1$), subsidence is medium, and in class 3 ($U < 0.9$), subsidence is very high. However, in this study, we adopted the classification of Sinha-Roy (2002). In the Mougoué sub-basin, the U is 1.005 and relates to class 1 ($U \geq 1$), which tells us that there was a very high tectonic uplift in this section of the study area. In the Mélangué and Lokoundjé sub-basins and in the Nyong basin, the values of U are respectively around 0.99, 0.96, and 0.84 and are found in the interval ($0.70 \leq U < 1.00$); therefore, these sub-basins and basin have recorded a high tectonic uplift that fits into class 2 (Fig. 6c). Class 3 ($U < 0.70$) materialising moderate to weak tectonic uplift and slight subsidence was not recorded in the study area.

Longitudinal Profiles (PL), knick-points (Kp)

The analysis of the longitudinal profiles (PL) of the rivers shows that the hydrographic network of the study area, although old, has not yet reached its state of dynamic equilibrium (Fig. 7) and vary from one watershed to another by their morphology according to their shape, slope, and the Kp occurrence (Fig. 7). These profiles display well-graded concave-, concavoconvex- and S-shape profiles. The Mougoué, Lokoundjé, and Mélangué PL are stepwise and have numerous projections varying between 10 and 20 m (Fig. 7e-g). The PL of the Nyong catchment area (Mvoulé 1, Mvoulé 2, Nkouambpoer) are concave and convex, with many large projections exceeding 200 m in places (Fig. 7a,b), and others are stepped steps whose projections exceed 150 m in places (Fig. 7c,d). Upstream the theoretical profiles are below the real profiles materialising a weak differential erosion, but downstream we note the opposite, marking a strong differential erosion (Fig. 7). In both cases, the dominant morphology is that of stairs with many breaks in slope (knick-points -kp-; Fig. 7). This stepwise evolution can be interpreted as the recording by watercourses of a series of reactivations of a system partially in equilibrium. The kp are due either to a variation of the lithology (Hack, 1973; Miller, 1991; Goldrick & Bishop, 1995; Wobus et al., 2006; Kirby & Whipple, 2012), either to an erosive imbalance following a

fall in the base level (Hack, 1973; Gardner, 1983; Seidl & Dietrich, 1992; Goldrick & Bishop, 1995), either the presence of an active fault scarp or simply an active deformation zone (Reed, 1981; Seeber & Gornitz, 1983) or to an increase in the erosive capacity at the junction of the tributaries (Seidl & Dietrich, 1992). By comparing the spatial distribution of kp with the lithological map (Fig. 1c), we found that some kp from Nkouambpoer, Mougué, Lokoundjé, and Mélangué are located at lithological boundaries, suggesting their relationship with changes in rock strength. All the other kp recorded do not seem to be linked to changes in lithology but either to the combined expression of active tectonic processes (faults and scarps) and the roughnesses developed on the stepped relief due to active differential erosion.

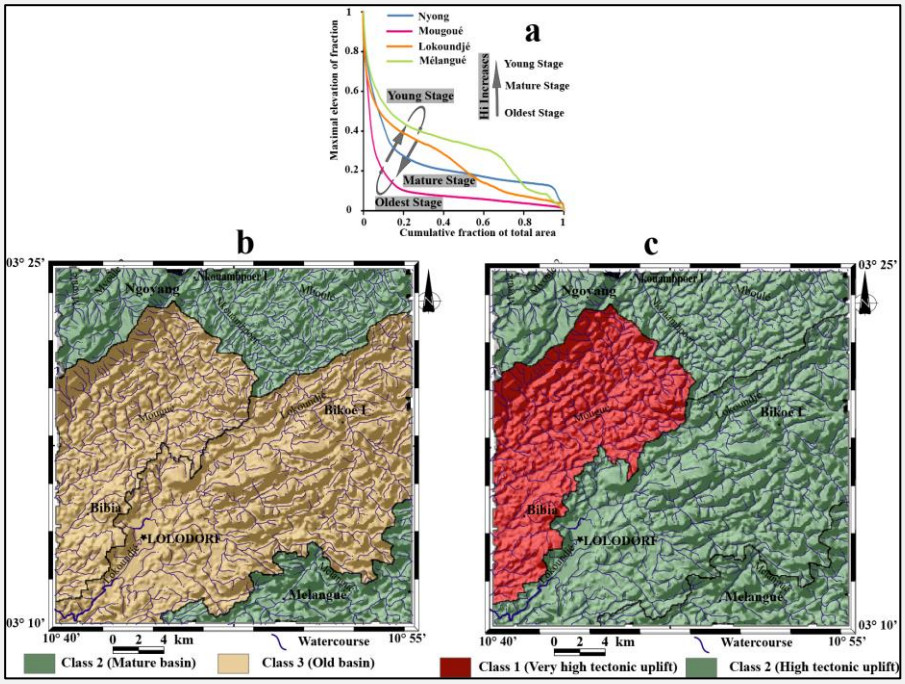

Figure 6. a) Hypsometric curves of the Lokoundjé and Nyong basins showing atypical forms indicative of their reactivations in the Lolodorf region and its surroundings. - Nyong, Lokoundjé and Mélangué illustrate the hypsometric curves at the mature stages and - Mougoué represents a hypsometric curve at the old stages; b) Classification map of the hypsometric integral values of the Lokoundjé and Nyong watersheds according to Anand & Pradhan (2019) in the Lolodorf region and its surroundings; c) Map representing the distribution of classes of relative tectonic uplifts of the Lokoundjé and Nyong basins according to Sinha-Roy (2002) in the Lolodorf region and its surroundings.

Stream length gradient index (SL-index)

The flow length gradient (SL-index) index developed by Hack (1973) measures the effect of relative tectonic activity in a watershed. SL-index determines local uplift and includes the incipient local response in the basin or sub-basin to regional tectonic events (Keller & Pinter, 1996, 2002; Troiani & Della-Seta, 2008). SL-index values have been calculated along major river lengths to support the identification of kp (failure) in Figure 7 and are graphically represented in Figure 8. According to Das (2018) who showed that SL-index curve peaks correspond to knick-zones and/or Kp anomalies, our peaks have a good number of Kp. According to Selby (1980), the Lolodorf rock hardness includes moderate, high and very high. In this work, the SL-index of Nyong (Nkouambpoer), Mougoué, Lokoundjé, and Mélangué are respectively around 20.18; 18.15; 24.49; and 39.10. These results fit into class 3 (SL-index < 300), which corresponds to weak or minor ancient tectonic activity. However, class 1 (SL-index > 500) and class 2 (300 ≤ SL-index < 500) are absent and correspond respectively to the predominant ancient tectonic activities (high) and to the average or moderate ancient tectonic activities (El Hamdouni et al., 2008).

Swath profile

All the windrow profiles in the Lolodorf sector and its surroundings show a decrease in altitude from inland towards the outlet (Fig. 9). Parallel to the profiles of Mvoulé 1 and Mvoulé 2, the altitude changes gradually, while the profiles of Nkouambpoer, Mboulé, Mougoué, Lekoundjé, and Mélangué have altitudes that change abruptly, say, a rapid increase in altitude to about 620 m (Figs. 9c-d, 9e-g) followed by a sharp drop. The Lokoundjé windrow profiles (average and maximum) are almost superimposed along their route, but in the Mougoué and Mélangué sectors, they are also overlapped in certain places (Fig. 9e-g).

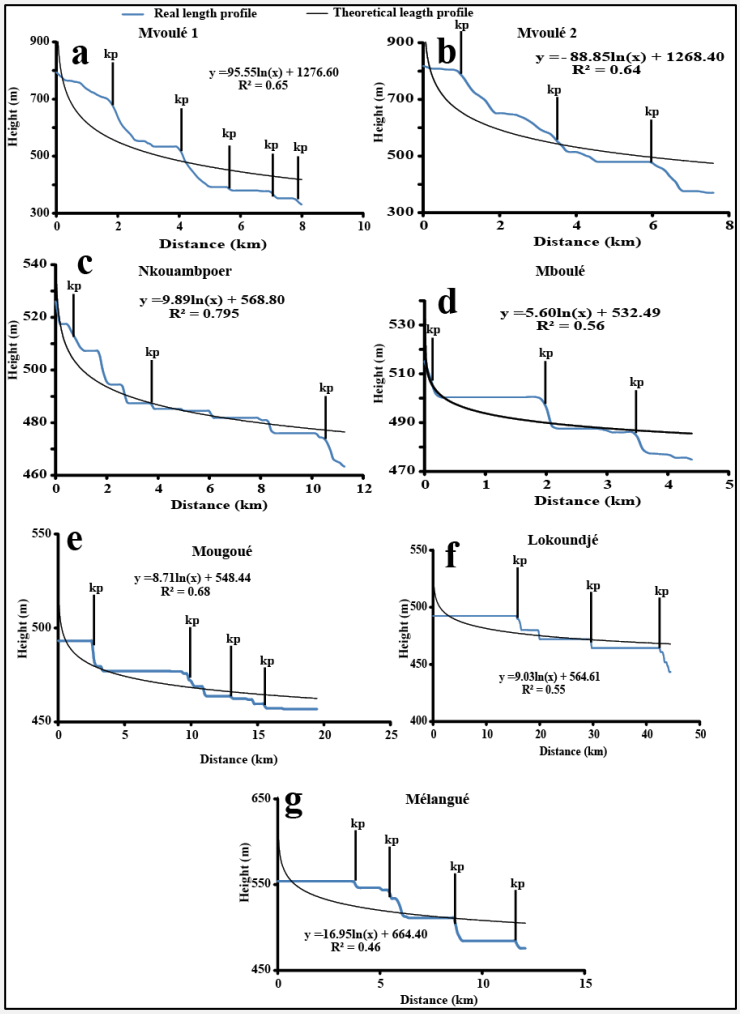

Figure 7. Real longitudinal profiles of the Nyong basin (a-d) and the Lokoundjé basin (e-g) compared to theoretical equilibrium profiles of the Lolodorf region and its surroundings.

Asymmetrie factor (AF)

The asymmetry factor (AF) makes it possible to evaluate the tectonic inclination or tilting of at the scale of a watershed and is applicable over a relatively large area (Hare & Gardner, 1985; Siddiqui & Soldati, 2014; Kale et al., 2014; Keller & Pinter, 2002).

The Mélangué sub-basin is asymmetrical with a tectonic tilt that occurred from left to right. It is class 1 (AF ≥ 15), with AF = 23.79 characterising very active tectonic activity. On the other hand, the sub-basin of the Mougoué has asymmetry and a moderate tectonic inclination due to an active tectonic activity, which fits into class 2, because the calculated AF is 13.90; it is included in the interval (10 ≤ AF < 15). For the Lokoundjé subbasin, the calculated AF is 7.50 and is found in the interval (5 ≤ AF< 10) of class 3. The tectonic inclination is weak due to a semi-active tectonic activity, and the stream is located in the center of the watershed. The Nyong basin is class 4 with an AF of around 2.09 (AF < 5) with

almost zero tectonic inclination (tectonically inactive). The watercourse is also located in the center of the watershed (Fig. 10a).

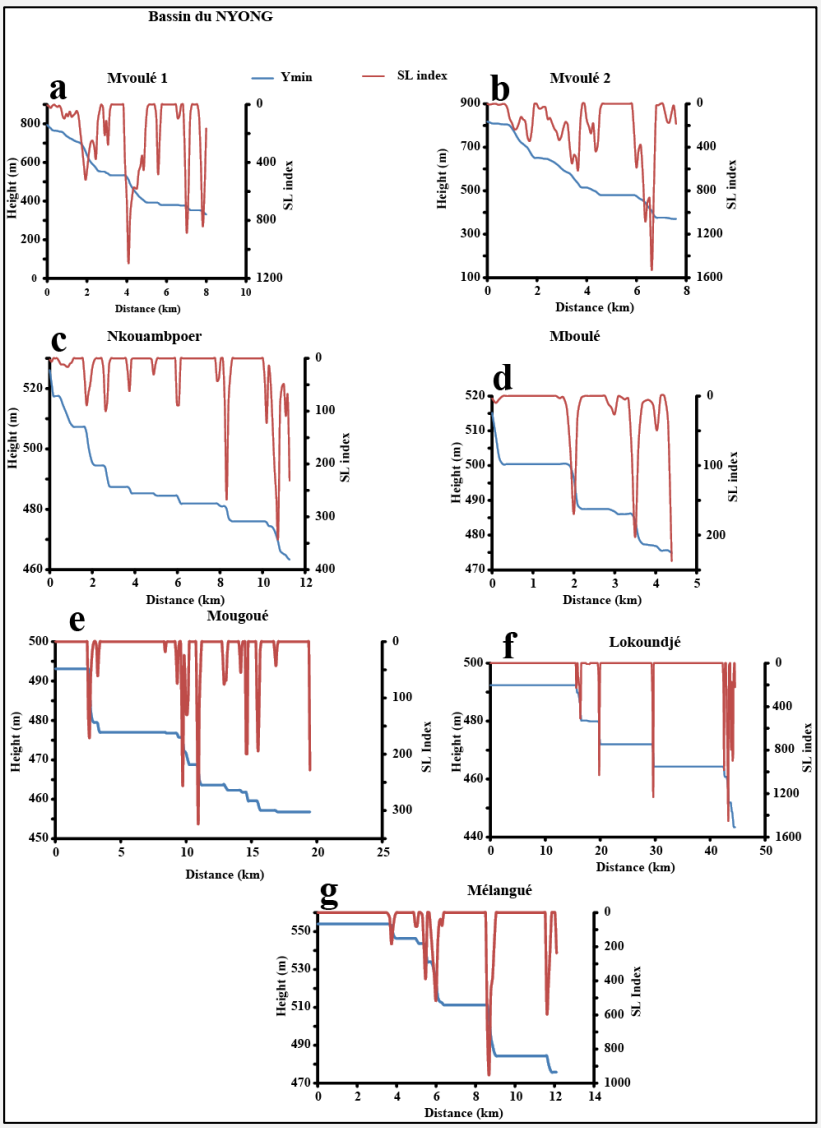

Figure 8. Stream length index (SL-index) of the Nyong basin (a-d) of the Lokoundjé basin (e-g) in the Lolodorf region and its surroundings.

Transverse topographic symmetric factor (TTSF)

The transverse topographic symmetry factor (TTSF) is used to assess the tilt related to neotectonic activity in a basin and the degree and variation of asymmetry in different portions of the valley (Alipoor et al., 2011). In the Nyong basin, the T is equal to 0.55, and in that of the Lokoundjé it is 0.50, which reflects class 1 ($T \geq 0.4$) corresponding to high neotectonic activity or high tectonic activity (Keller & Pinter, 1996; El Hamdouni et al., 2008). The Mougoué and Mélangué basins are class 2 ($0.20 < T < 0.40$), with T of the order of 0.22 and 0.38 due to moderate neotectonic activity or simply qualified as moderate tectonic activity (Fig. 10b; Keller & Pinter, 1996; El Hamdouni et al., 2008). Class 3 ($T \leq 0.2$) characterising low neotectonic activity or simply low tectonic activity (Keller & Pinter, 1996; El Hamdouni et al., 2008) is not listed in the study area. In the Nyong and Lokoundjé basins, the TTSF tends towards zero, inducing a symmetrical basin. On the other hand, in the Mougoué and Mélangué basins, the TTSF increases towards 1, reflecting an increasing asymmetry. It illustrates the tilting of stream channels due to possible basin movement caused by variations in slope polarity and bedrock influence that are insignificant on-stream migration.

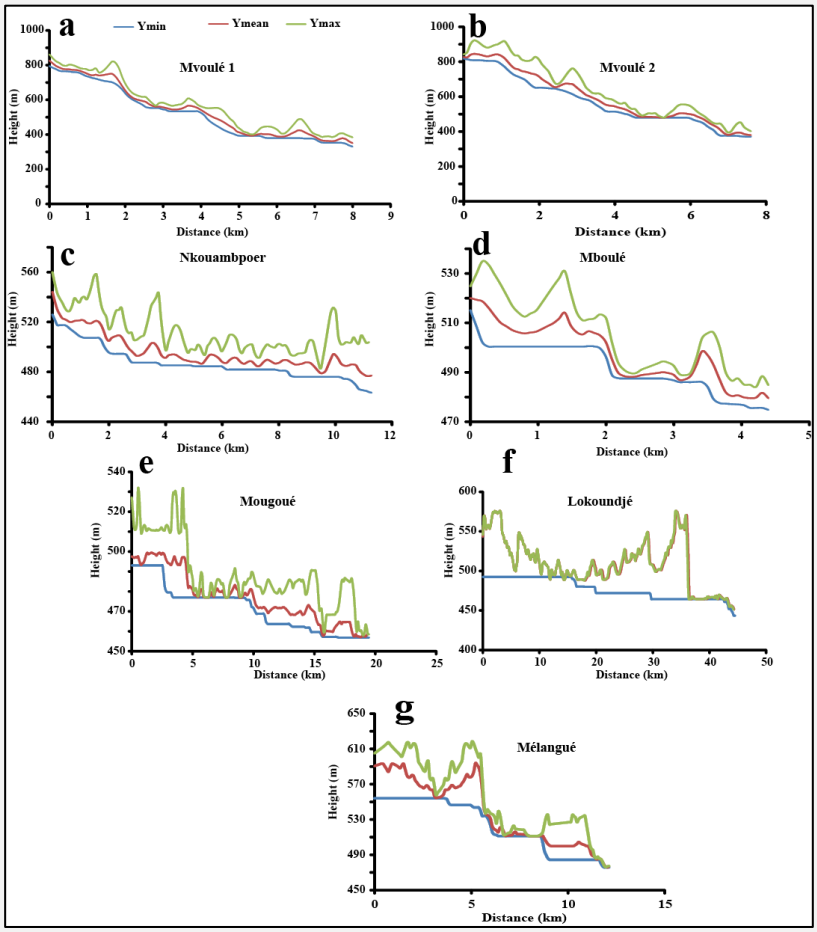

Figure 9. Swath profile of the Nyong basin (a-d) of the Lokoundjé basin (e-g) in the Lolodorf region and its surroundings.

Basin shape (Bs)

The shape of the basin (Bs) is used to determine whether or not tectonic effects are controlled or the morphological characteristics (stretched or circular) of the basin (Ramírez-Herrera, 1998). The Nyong watershed is class 1 (Bs > 4) because it has a Bs of around 4.26, which denotes its elongation under very high tectonic effects. However, in the Lokoundjé and Mélangué basins, the Bs have respective values of around 3.21 and 3.14, which characterise class 2 ($3 \leq Bs \leq 4$). These basins are moderately circular and have been subjected to moderate tectonics; on the other hand, the Mougoué basin is more circular than the previous basins and has recorded relatively weak tectonics with a Bs of around 2.55 illustrating class 3 (Bs < 3; Fig. 10c; El Hamdouni et al., 2008).

Relative tectonic activity (Iat)

The relative tectonic activity (Iat) is a geomorphological parameter that is a function of the other parameters studied above. The Mélangué basin has an Iat of around 2 (class 2; 1.5 < Iat < 2), highlighting the predominance of high tectonic activity. On the other hand, in the Nyong, Lokoundjé, and Mougoué basins, the Iat has in turn values of the order of 2.17 and 2.33 in the last two, characterising class 3 (2 < Iat < 2.5) showing moderate tectonic activity (Fig. 10d; El Hamdouni et al., 2008). Class 1 (1< Iat <1.5) and class 4 (Iat > 2.5) designate successively very high and low tectonic activities that are not recorded in the Lolodorf region and its surroundings (El Hamdouni et al., 2008).

These geomorphological parameters are expressed on the geological structures which were put in place under the effect of the geological constraints which we will address in this part of the work.

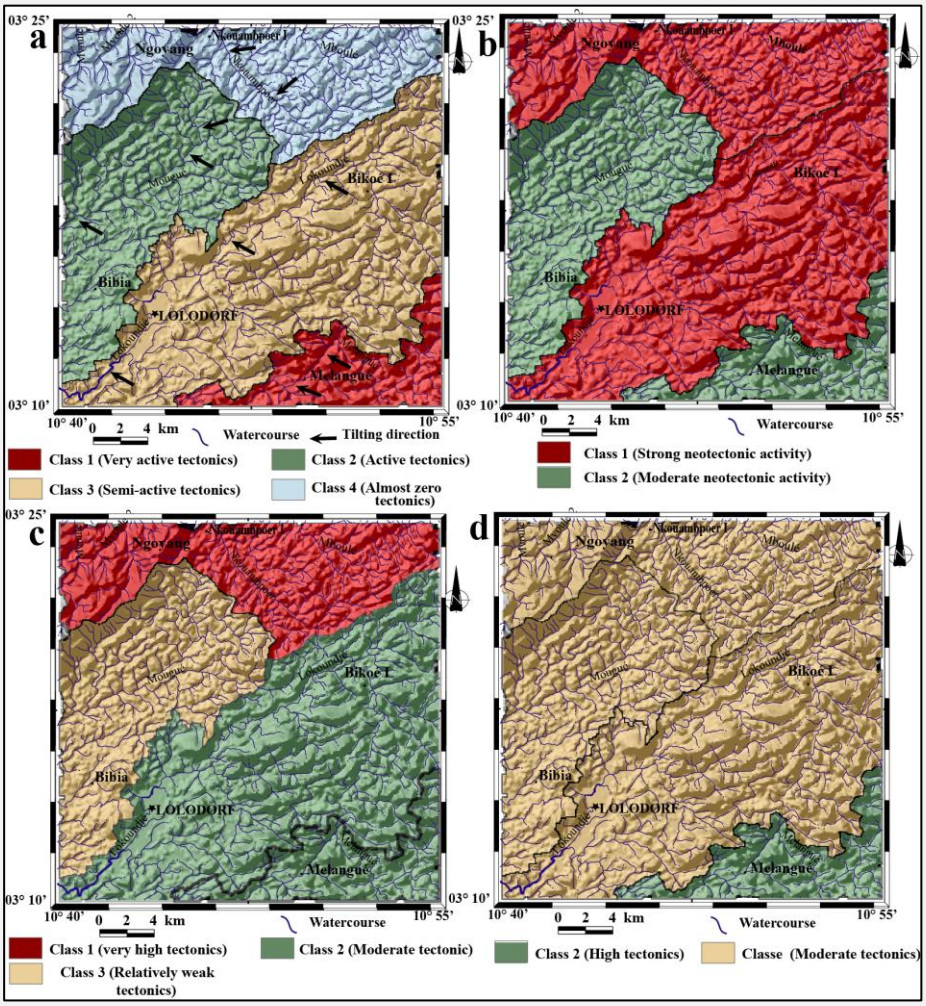

Figure 10. a) Map representing the distribution of Asymetrie factor (AF) of the Lokoundjé and Nyong basins according to Keller & Pinter (2002); b) Map representing the Transverse topographic symmetric factor (T) distribution of the Lokoundjé and Nyong basins according to Keller & Pinter (1996) and El Hamdouni et al. (2008); c) Map representing the Basin shape (Bs) distribution of the Lokoundjé and Nyong basins according to El Hamdouni et al. (2008); d) Map representing the Relative tectonic activity (Iat) distribution of the Lokoundjé and Nyong basins according to El Hamdouni et al. (2008).

DISCUSSION

The pre-existing Proterozoic tectonic features control the present-day geomorphology. In this study the main goal is to analyse, evaluate, and quantify the role of active tectonics in the zone Lolodorf and surrounding area. The assessment of relative tectonic activity in the past has been done using a limited number of geomorphic indices (Messi Ottou et al., 2014a). The investigation of the present study is to decipher active tectonism in the same area using linear, areal, relief parameters with geomorphic indices and field data.

The study area is a vast depression full of rectilinear V- and U-shaped valleys, and the incision of the valleys, eroded valleys bordered by two plateaus of different amplitudes: to the north, the Ngovayang range, which culminates at 1100 m altitude, and to the south, the Mvengué hills, whose altitude maximum is of the order of 940 m. The respective contacts between the two morphological entities (plateaus and depression) are scarps (faults) visible both on the ground and on satellite images: the scarps (faults) of Ngovayang and Lokoundjé. These characteristics could be the origin of the morphology of the Douala-Buea (Balla Ateba et al., 2021), Bafoussam and Mamfe (Wabo Defo et al., 2022), and Garoua-Gaschiga (Mvondo Owono et al., 2024) regions. These tectonic features also control hydrographic patterns dominated by rectangular and parallel trends (Mvondo Owono et al., 2024). The

escarpment (fault) of the Lokoundjé guides the river whose name it bears. The two escarpments (faults) are almost parallel, and the entities they delimit have a NE-SW orientation, reminiscent of that of the Sanaga fault or the Bénoué ditch parallel to the orographic and hydrographic lineaments (Dumont, 1986; Owona et al., 2011; Wabo Defo et al., 2022; Mvondo Owono et al., 2024). They affect, in the same way as the Sanaga fault, very old formations (> 600 Ma); they are all at least post-Eburnean (Owona et al., 2011). The morphology and spatial arrangement of the three morphological units (I, II and III) on one hand and the opposition of the scarps (faults) of the Lokoundjé and the Ngovayang on the other hand, indicate that the region of Lolodorf and its surroundings is a grabben/ditch of collapse which would have been set up during the formation or the replay of the scarps (faults) of the Lokoundjé and the Ngovayang (Messi Ottou et al., 2014a). Themselves consecutive to a continental uplift illustrated by abrupt hypsometric curves at the base (Fig. 6a) and a very high tectonic uplift to raise (Fig. 10d) produced by a weak or minor old tectonic activity (Sinha-Roy, 2002).

By comparing the rosettes of Figure 5a,b, we note that the field results are superimposable with the laboratory results, thus demonstrating the reliability of the lineament extraction method by photo-interpretation. In addition, all the observations of the regional folds indicate a WNW-ESE, E-W and NNW-SSE compression in an extensive and strike-slip regime in the region (Messi Ottou et al., 2014a,b). This assertion is in the same direction as Vidal et al. (1996) who mentioned a set of strike-slip faults in the Paleoproterozoic domain of the Northeast of Côte d'Ivoire. The geomorphological indices applied highlight the different tectonic processes that have shaped the landscape of the study area.

Longitudinal profiles, hypsometric curves and normalized stream profiles inform on heterogeneous and unequally tectonic activities and erosion processes (Bull & McFadden, 1977; Burbank & Anderson, 2001; Keller & Pinter, 2002). The convex hypsometric curves characterise young and slightly eroded regions; S-shaped curves represent moderately eroded regions; and concave curves represent heavily eroded regions (Pedrera et al., 2009). Convex curves are dominant in materialising slightly eroded bedrock, strongly fractured due to structural discontinuities that cross the different basins. They infer active tectonic activity close to its equilibrium stage and reflect controlled lithological and structural heterogeneities (Hack, 1957; Burbank & Anderson, 2001; Keller & Pinter, 2002; Pérez-Peña et al., 2010; Matoš et al., 2014). The range of upper to lower values of the Hi suggests that a large amount of rock mass is undergoing a process of denudation while many materials have been eroded (El Hamdouni et al., 2008). High-altitude, low-relief surfaces contribute to tectonic disturbances in the basin. The values of the hypsometric integral vary between 0.06 and 0.35; the higher values are assigned to the curves of convex shape, while the lower values represent the curves of concave shape (Fig. 6a; Ali & Ikbal, 2020). The lower Hi values in the Mougoué and Lokoundjé basins are the consequence of runoff dissecting the landscape due to the high kinetic energy, which increases erosive activity (Shukla et al., 2014).

Substantial displacement of the watershed results from tectonic activities. The Mélangué sub-basin belongs to Class 1 located SE of the study area; it underwent a shift towards the NW due to high tectonic activity over an area of 73.34 km^2, which would be a cratonic portion. The study area comprises 10% (Class 1), 26% (188.35 km^2, Class 2), 34% (263.25 km^2, Class 3) and 30% (168.03 km^2, Class 4) (Fig. 10a). The result obtained from the analysis of the asymmetry factors results from the large-scale tilting phenomena that could be due to the passage of thrusts or faults of the Lokoundje, Ngovayang, and Nyong crossing the basins. Like the Sanaga fault or the Bénoué ditch, they have been reactivated several times over time (Ngako et al., 2003; Njonfang et al., 2008). The pre-existing fractures reactivated in a privileged network consisting of faults orientated N 30 to N 60 (Allix & Popoff, 1983; Regnoult, 1983; Benkhelil, 1998) to which belong the scarps (faults) of the Ngovayang and the Lokoundjé and other lineaments which have the directions of the major tectonic lineaments of Cameroon (Cameroon Volcanic Line (CVL) N025 to N040, of the Sanaga and that of the Adamaoua N065 to N070) and sub-regional directions ("Cameroon-Gabon" N005 to N015 and those of the Gulf of Guinea N105 to N145) (Dumont, 1986; Thierry et al., 2006), which are well marked by their layout and therefore influence the hydrographic system of the region (Fig. 5a).

The stream-length gradient index and the actual river profile indicate that there is an increase in the value of SL-index near tectonically active areas. SL-index anomalies identified along our river profiles correlate sometimes with faults, sometimes with lithological contact between metamafites, charnockitic gneisses, migmatitic gneisses and clinopyroxene metasyenites (Fig. 1c). These SL-index anomalies appear as good indicators of active structures (Kirby et al., 2003; Kirby & Ouimet, 2011; Ambili & Narayana, 2014; Gaidzik & Ramírez-Herrera, 2017; Nsangou Ngapna et al., 2020). The values of the SL-index show abnormal behaviour when passing through the Nyong and Lokoundjé basins at the level of watercourses such as Mvoulé 1 and 2, Nkouambpoer and Mboulé (Fig. 8a-d), Mougoué, Lokoundjé, and Mixed (Fig.

8e-g) and lithological variations. The values of the SL-index calculated for each basin were classified into old weak or minor tectonic zones. These basins are crossed by two major scarps (faults) with variable lithological contrasts having recorded tectonic disturbances within them. Higher SL-index values on a lithology suggest variable thrusts due to tectonic control (Sharma et al., 2018). Lower SL-index values represent when streams cross strike-slip faults (Dehbozorgi et al., 2010). There are different views regarding an increase in SL-index values regarding lithology variability and tectonic activities. Harkins et al. (2005) suggested that SL-index values increase in more resistant bedrock. However, Brookfield (1998) suggested that tectonic activities induce higher values of SL-index. The increase in the SL-index values of this study area would result from tectonic disturbances as well as from the lithological contrast (Fig. 8).

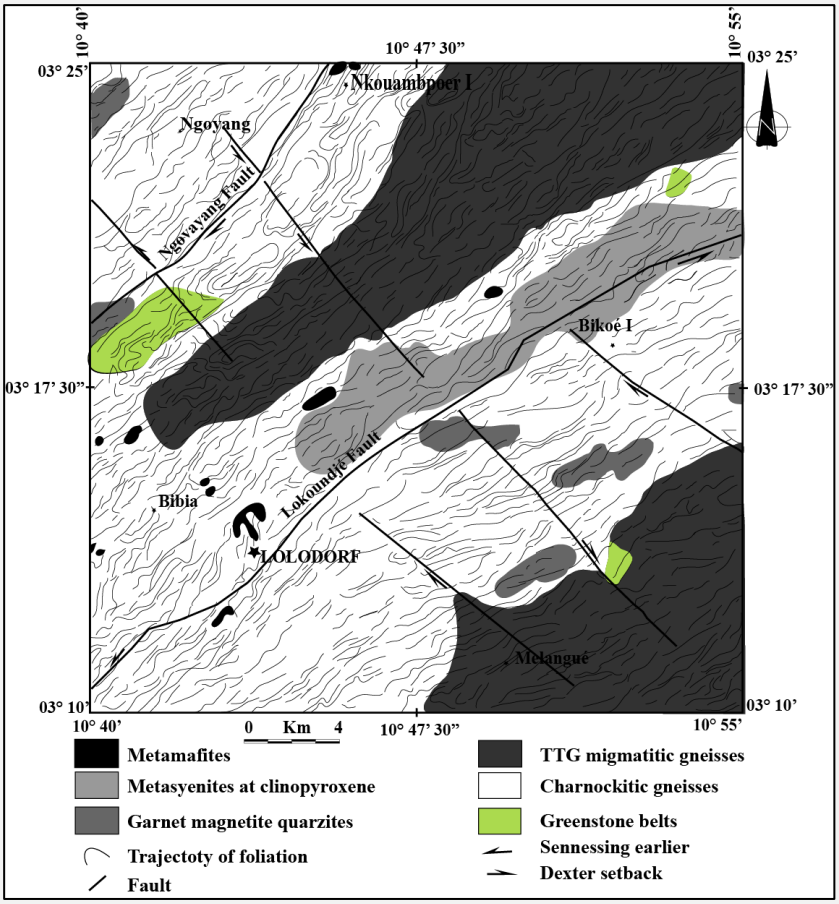

Figure 11. Geological map of the Lolodorf area and its surroundings.

The basin shape index was interpreted to determine the influence of tectonic activity. The Nyong basin has been elongated under very high tectonic effects and covers an area of 168.03 km2, while the Lokoundjé and Mélangué basins cover areas of 263.25 km^2 and 73.34 km^2, respectively, under a moderate tectonic activity, and that of Mougoué (188.35 km^2) has relatively low tectonic activity (Fig. 10c).

The average of linear parameters, surface relief, and geomorphological indices were used to assess the spatial distribution of relative tectonic activity in the study area. Iat values have been grouped into two classes based on tectonic activity (El Hamdouni et al., 2008). The distribution of Iat classes has been classified into class 2 reflecting relative tectonic activity (1.5 < Iat < 2) and class 3 materialising moderate tectonic activity (2 < Iat < 2.5) based on the tectonic activities. The spatial distribution of Iat is shown in Figure 10d. Results interpreted from Iat had already been validated by a previous study that predicted strong and moderate neotectonic activities that would lead to landslide activation and other natural hazards (Fig. 7; Messi Ottou et al., 2014b). These parameters had been evaluated to determine the decisive factors for the increase of geohazards in the area.

These different geometries are proofs of a tectonic instability (Kp) that can be explained by the fact that, each time the basin tends towards maturity, it is rejuvenated by tectonics (installation of a fault or reactivation of an old fault), which creates the slope and thereby resets the work of erosion. These Kp can be related either to lithological contacts or faults. To this must be added the lithological component (Fig. 11) because the contrasting competence of the geological formations of the region makes differential erosion locally very variable, setting up dissected and mature drainage basins resulting from extensive erosion in the peneplains, dips with straight to moderately circular vergence (Fig. 6b; Anand & Pradhan, 2019). In addition, we have circular drainage basins with moderate and asymmetrical inclination. These two drainage basins have alternately recorded moderate and weak neotectonic activity (Fig. 10b,c; Keller & Pinter, 1996; El Hamdouni et al., 2008); on the other hand, the elongated basins have almost zero inclinations due to a high tectonic activity (Keller & Pinter, 1996; El Hamdouni et al., 2008).

CONCLUSION

The morphometric parameters (linear and relief parameters) and geomorphological indicators in the Lolodorf region emphasise the importance of active tectonics in the Nyong and Lokoundjé River basins. Additionally, satellite imagery, the worldwide spatial distribution of the lithological types and their limits, orography, and hydrography are used to expose it. These parameters have been selected to analyse the neotectonic activities in the region. The incorporation of linear, areal, and relief parameters with geomorphic indices acts as a significant tool for the Relative Tectonic Activity Index (Iat), as it shows a strong correlation with structural discontinuities and geomorphological anomalies. The approach helps in the identification of tectonically active zones. The values of asymmetric factors of different basins define that basin have structural discontinuity and are passing through major faults and thrusts. The anomalous values Hi, the SL-index is representative that most of the basins are subjected to active erosional processes or have significant tectonic disturbances. Higher values of Bs are also determinant factors for active tectonism in the study area. The combination of all those parameters with linear, areal, and relief parameters will help in determining the Iat.

The topographical variations allowed us to subdivide the area of Lolodorf and its surroundings into three levels or domains and to highlight three main morphological units: (a) the low unit (altitudes below 570 m) constitutes the vast Lolodorf depression; (b) the medium unit (570 < altitude < 800 m) is a high plateau dissected by deep valleys that individualise NE-SW-orientated Mvengué hills to E-W; and (c) the high unit chain (altitude > 800 m), which is an elliptical hill whose major axis is orientated NE-SW.

The alignment and spatial arrangement of steep slopes, low slopes, and the variable resistance of erosion attest to the tectonic control of geomorphology. In addition, the rugosities developed on the stepped relief indicate that differential erosion simultaneously controls tectonics and lithology.

The dendritic nature of this network indicates that it is developed on an impermeable base. While it's parallel and angular tendencies testify to its tectonic control (geological). The deep nature of the valleys that house this hydrographic network indicates the major role of run-off water in their degradation. Most kp are the combined expression of faults and lithological changes.

It is possible to generalise the aforementioned active lithological and tectonic controls on the Paleoproterozoic landscape of the Lolodorf region to the entire NyC. Additionally, they draw attention to its uniqueness throughout the entirety of southwest Cameroon, as well as the Paleoproterozoic terrains of Cameroon and even the equatorial border of West Africa.

ACKNOWLEDGEMENTS

We warmly thank the anonymous reviewers who have raised the quality of this article and all the staff of the School of Geology and Mining of the University of Ngaoundéré in Meiganga who have supported me since my arrival in this school.

REFERENCES

Abeng, S. A. E., Ndjigui, P. D., Beyanu, A. A., Teutsong, T., & Bilong, P. (2012). Geochemistry of pyroxenites, amphibolites and their weathered products in the Nyong unit, SW Cameroon (NW border of Congo craton): Implications for Au–PGE exploration. *Journal of Geochemical Exploration, 114*, 1-19. https://doi.org/10.1016/j.gexplo.2011.11.003

Aju, C. D., Reghunath, R., Achu, A. L., & Rajaneesh, A. (2022). Understanding the hydrogeochemical processes and physical parameters controlling the groundwater chemistry of a tropical river basin, South India. *Environmental Science and Pollution Research, 29*(16), 23561-23577. https://doi.org/10.1007/s11356-021-17455-w

Ali, S. A., & Ikbal, J. (2020). Assessment of relative active tectonics in parts of Aravalli mountain range, India: implication of geomorphic indices, remote sensing, and GIS. *Arabian Journal of Geosciences, 13*(2), 57. https://doi.org/10.1007/s12517-019-5028-2

Alipoor, R., Poorkermani, M., Zare, M., El Hamdouni, R. (2011). Active tectonic assessment around Rudhar Lorestan dam site, high Zagros Belt (SW of Iran). *Geomorphology 128*(1-2), 1-14. http://dx.doi.org/10.1016/j.geomorph.2010.10.014

Allix, P., & Popoff, M. (1983). Approche géodynamique du fossé de la Bénoué (NE Nigéria) à partir des données de terrain et de télédétection. *Bulletin Centre de Recherche Exploration Production Elf-Aquitaine, 7*(1), 323-337.

Ambili, V., & Narayana, A. C. (2014). Tectonic effects on the longitudinal profiles of the Chaliyar River and its tributaries, southwest India. *Geomorphology, 217*, 37-47. https://doi.org/10.1016/j.geomorph.2014.04.013

Anand, A. K., & Pradhan, S. P. (2019). Assessment of active tectonics from geomorphic indices and morphometric parameters in part of Ganga basin. *Journal of Mountain Science, 16*(8), 1943-1961. https://doi.org/10.1007/s11629-018-5172-2

Balla Ateba, C., Owona, S., Nsangou Ngapna, M., Manga Tsimi, V., Minyem, D., & Mvondo Ondoa, J. (2021). Lithostructural controls in Douala-Buea Region landscape (SW Cameroon margin): Insights from morphometric analysis. *Journal of Mountain Science, 18*(1), 68-87. https://doi.org/10.1007/s11629-020-6085-4

Benkhelil, J. (1998). Structure et évolution géodynamique du basin bassin intracontinental de la Bénoué (Nigéria). *Bulletin Centre de Recherche Exploration Production Elf-Aquitaine, 12*, 29-128.

Bouyo, M. H., Penaye, J., Mouri, H., & Toteu, S. F. (2019). Eclogite facies metabasites from the Paleoproterozoic Nyong Group, SW Cameroon: mineralogical evidence and implications for a high-pressure metamorphism related to a subduction zone at the NW margin of the Archean Congo craton. *Journal of African Earth Sciences, 149*, 215-234. https://doi.org/10.1016/j.jafrearsci.2018.08.010

Brookfield, M. E. (1998). The evolution of the great river systems of southern Asia during the Cenozoic India Asia collision: rivers draining southwards. *Geomorphology, 22*(3-4), 285-312. https://doi.org/10.1016/S0169-555X(97)00082-2

Bull, W. B. (2007). *Tectonic geomorphology of mountains: a new approach to paleoseismology*. John Wiley & Sons.

Bull, W. B., & McFadden, L. D. (2020). Tectonic geomorphology north and south of the Garlock fault, California. In *Geomorphology in arid regions* (pp. 115-138). Routledge.

Burbank, D. W., & Anderson, R. S. (2001). *Tectonic geomorphology*. Blackwell Science.

Cox, R. T. (1994). Analysis of drainage-basin symmetry as a rapid technique to identify areas of possible Quaternary tilt-block tectonics: an example from the Mississippi Embayment. *Geological Society of America Bulletin, 106*(5), 571-581. https://doi.org/10.1130/00167606(1994)106<0571:AODBSA>2.3.CO;2

Das, S. (2018). Geomorphic characteristics of a bedrock river inferred from drainage quantification, longitudinal profile, knickzone identification and concavity analysis: a DEM based study. *Arabian Journal of Geosciences, 11*(21), 680. https://doi.org/10.1007/s12517-018-4039-8

Deffontaines, B., & Chorowicz, J. (1991). Principle of drainage basin analysis from multisource data. Application to the structural analysis of the Zair basin. *Tectonophysics, 194*(3), 237-263. https://doi.org/10.1016/0040-1951(91)90263-R

Dehbozorgi, M., Pourkermani, M., Arian, M., Matkan, A. A., Motamedi, H., & Hosseiniasl, A. (2010). Geomorphology Quantitative analysis of relative tectonic activity in the Sarvestan area, central Zagros, Iran. *Geomorphology, 121*(3), 329-341. https://doi.org/10.1016/j.geomorph.2010.05.002

Dumont, J. F. (1986). Identification par télédétection de l'accident de la Sanaga (Cameroun). Sa position dans le contexte des grands accidents d'Afrique Centrale et de la limite nord du craton congolais. *Géodynamique, 1*(1), 13-19.

El Hamdouni, R.., Irigaray, C., Fernández, T., Chacón J., & Keller, E. A. (2008). Assessment of relative active tectonics, southwest border of the Sierra Nevada (southern Spain). *Geomorphology, 96*(1-2), 150-173. https://doi.org/10.1016/j.geomorph.2007.08.004

Eynoddin, E. H., Solgi, A., Pourkermani, M., Matkan, A., & Arian, M. (2017). Assessment of relative active tectonics in the Bozgoush Basin (SW of Caspian Sea). *Open Journal Marine Sciences, 7*(2), 211-237. https://doi.org/10.4236/ojms.2017.72016

Feybesse, J. L., Johan, V., Triboulet, C., Guerrot, C., Mayaga-Mikolo, F., Bouchot, V., & N'dong, J. E. (1998). The West Central African belt: a model of 2.5–2.0 Ga accretion and two-phase orogenic evolution. *Precambrian research, 87*(3-4), 161-216. https://doi.org/10.1016/S0301-9268(97)00053-3

Figueiredo, P. M., Rockwell, T. K., Cabral, J., & Lira, C. P. (2019). Morphotectonics in a low tectonic rate area: analysis of the southern Portuguese Atlantic coastal region. *Geomorphology, 326*, 132-151. https://doi.org/10.1016/j.geomorph.2018.02.019

Gaidzik, K., & Ramírez-Herrera, M. T. (2017). Geomorphic indices and relative tectonic uplift in the Guerrero sector of the Mexican forearc. *Geoscience Frontiers, 8*(4), 885-902. https://doi.org/10.1016/j.gsf.2016.07.006

Gardner, T. W. (1983). Experimental study of knickpoint and longitudinal profile evolution in cohesive, homogeneous material. *Geological Society of America Bulletin, 94*(5), 664-672. https://doi.org/10.1130/0016-7606(1983)94%3C664:ESOKAL%3E2.0.CO;2

Goldrick, G., & Bishop, P. (1995). Differentiating the roles of lithology and uplift in steepening bedrock river long profiles: an example from Southeastern Australia. *Journal of Geology, 103*, 227-231. https://doi.org/10.1086/629738

Hack, J. T. (1973). Stream-profile analysis and stream-gradient index. *Journal of Research of the us Geological Survey, 1*(4), 421-429.

Hare, P. W., & Gardner, T. W. (1985). Geomorphic indicators of vertical neotectonism along converging plate margins, Nicoya Peninsula, Costa Rica. In: Morisawa M. & Hack J.T. (Eds.), Tectonic Geomorphology. *Proceedings of the 15th Annual Bighamton Geomorphology Symposium*. Allen & Unwin, Boston, 75-104.

Harkins, N. W., Anastasio, D. J., & Pazzaglia, F. J. (2005). Tectonic geomorphology of the Red Rock fault, insights into segmentation and landscape evolution of a developing range front normal fault. *Journal of Structural Geology, 27*(11), 1925- 1939. https://doi.org/10.1016/j.jsg.2005.07.005

Harlin, J. M. (1978). Statistical moments of the hypsometric curve and its density function. *Journal of the International Association for Mathematical Geology, 10*(1), 59-72. https://doi.org/10.1007/BF01033300

Huang, X., & Niemann, J. D. (2006). Modelling the potential impacts of groundwater hydrology on long-term drainage basin evolution. *Earth Surface Processes and Landforms: The Journal of the British Geomorphological Research Group, 31*(14), 1802-1823. https://doi.org/10.1002/esp.1369

Kale, V. S., Sengupta, S., Achyuthan, H., & Jaiswal, M. K. (2014). Tectonic controls upon Kaveri River drainage, cratonic Peninsular India: Inferences from longitudinal profiles, morphotectonic indices, hanging valleys and fluvial records. *Geomorphology, 227*, 153-165. https://doi.org/10.1016/j.geomorph.2013.07.027

Keller, E. A., & Pinter, N. (1996). *Active Tectonics: Earthquake, Uplift, and Landscape*. Prentice Hall.

Keller, E. A., & Pinter, N. (2002). *Active Tectonics: Earthquakes, Uplift, and Landscape (Second ed)*. Prentice Hall.

Kirby, E., & Ouimet, W. (2011). Tectonic geomorphology along the eastern margin of Tibet: insights into the pattern and processes of active deformation adjacent to the Sichuan Basin. In: Gloaguen, R., & Ratschbacher, L (Eds). *Growth and Collapse of the Tibetan Plateau*. Geological Society of London, Special Publications, 165-188. https://doi.org/10.1144/SP353.9

Kirby, E., & Whipple, K. X. (2012). Expression of active tectonics in erosional landscapes. *Journal of Structural Geology, 44*, 54-75. http://doi.org/10.1016/j.jsg.2012.07.009

Kirby, E., Whipple, K. X., Tang, W., & Chen, Z. (2003). Distribution of active rock uplift along the eastern margin of the Tibetan Plateau: Inferences from bedrock channel longitudinal profiles. *Journal of Geophysical Research: Solid Earth, 108*(B4). https://doi.org/10.1029/2001JB000861

Koukouvelas, I. K., Piper, D. J., Katsonopoulou, D., Kontopoulos, N., Verroios, S., Nikolakopoulos, K., & Zygouri, V. (2020). Earthquake-triggered landslides and mudflows: Was this the wave that engulfed Ancient Helike? *The Holocene, 30*(12), 1653-1668. https://doi.org/10.1177/0959683620950389

Koukouvelas, I. K., Zygouri, V., Nikolakopoulos, K., & Verroios, S. (2018). Treatise on the tectonic geomorphology of active faults: The significance of using a universal digital elevation model. *Journal of Structural Geology, 116*, 241-252. https://doi.org/10.1016/j.jsg.2018.06.007

Larue, J. P. (2008). Tectonic influences on the Quaternary drainage evolution on the north-western margin of the French Central Massif: The Creuse valley example. *Geomorphology, 93*(3-4), 398-420. http://doi.org/10.1016/j.geomorph.2006.11.014

Lerouge, C., Cocherie, A., Toteu, S. F., Penaye, J., Milesi, J. P., Tchameni, R., Nsifa, N. E., Fanning, C. M., & Deloule, E. (2006). SHRIMP U/Pb zircon age evidence for paleoproterozoic sedimentation and 2.05 Ga syntectonicplutonism in the Nyong Group, South-western Cameroon: consequences for the eburnean-transamazonian belt of NE Brasil and central Africa. *Journal of African Earth Sciences, 44*(4-5), 413-427. https://doi.org/10.1016/j.jafrearsci.2005.11.010

Lifton, N. A., & Chase, C. G. (1992). Tectonic, climatic and lithologic influences on landscape fractal dimension and hypsometry: implications for landscape evolution in the San Gabriel Mountains, California. *Geomorphology, 5*(1), 77-114. https://doi.org/10.1016/0169-555X(92)90059-W

Loose, D., & Schenk, V. (2018). 2.09 Ga old eclogites in the Eburnian-Transamazonian orogen of southern Cameroon: significance for Palaeoproterozoic plate tectonics. *Precambrian Research, 304*, 1-11. https://doi.org/10.1016/j.precamres.2017.10.018

Mahmood, S. A., & Gloaguen, R. (2012). Appraisal of active tectonics in Hindu Kush: insights from DEM derived geomorphic indices and drainage analysis. *Geosciences Frontier, 3*(4), 407-428. https://doi.org/10.1016/j.gsf.2011.12.002

Mathew, M. J. (2016). *Geomorphology and Morphotectonic Analysis of north Borneo* (Doctoral dissertation, Lorient).

Mathew, M. J., Menier, D., Siddiqui, N., Kumar, S. G., & Authemayou, C. (2016b). Active tectonic deformation along rejuvenated faults in tropical Borneo: inferences obtained from tectono-geomorphic evaluation. Geomorphology, 267, 1-15. https://doi.org/10.1016/j.geomorpho.2016.05.0176

Mathew, M. J., Menier, D., Siddiqui, N., Ramkumar, M., Santosh, M., Kumar, S., & Hassaan, M. (2016a). Drainage basin and topographic analysis of a tropical landscape: Insights into surface and tectonic processes in northern Borneo. *Journal of Asian Earth Sciences, 124*, 14-27. https://doi.org/10.1016/j.jseaes.2016.04.016

Matoš, B., Tomljenovic, B., & Trenc, N. (2014). Identification of tectonically active areas using DEM: a quantitative morphometric analysis of Mt. Medvednica, NW Croatia. *Geological quarterly, 58*(1), 51-70. https://doi.org/10.7306/gq.1130

Maurizot, P., Abessolo, A., Feybesse, J. L., Johan, V., & Lecomte, P. (1986). Etude et prospection minière du Sud-Ouest Cameroun. *Synthèse des travaux de*, 274.

Mayer, L. (1990*). Introduction to quantitative geomorphology*. Prentice Hall.

Messi Ottou, E. J., Ntomba, S. M., Bidzang, F. N., Akame, J. M., Owona, S., & Ondoa, J. M. (2014). Géomorphologie structurale et risque naturel dans une portion de zone mobile du complexe du Nyong au SW Cameroun: cas de la région Lolodorf-Mvengue. *Afrique Science: Revue Internationale des Sciences et Technologie, 10*(4), 288-298.

Messi Ottou, E. J., Ntomba, S. M., Ntieche, B., Magnekou Takamte, R. C., Bisse, S. B., Ndong Bidzang, F., & Mvondo Ondoa, J. (2022). Petrology of the meta-mafic rocks from the Lolodorf area, Nyong complex (Southwest Cameroon): implication for the origin and emplacement conditions. *SN Applied Sciences, 4*(8), 216. https://doi.org/10.1007/s42452-022-05089-7

Messi Ottou, E. J., Owona, S., Mvondo Owono, F., Ntomba, S. M., Akame J. M., Nsangou Ngapna, M., Koum, S., & Mvondo Ondoa, J. (2014). Analyse morphotectonique par couplage d'un modèle numérique de terrain (MNT) et des données de terrain d'une portion de zone mobile paléoprotérozoïque de la région de Lolodorf (Complexe du Nyong, SW Cameroun). *Sciences, Technologies et Développement, 15*, 9-25.

Miller, J. R. (1991). The influence of bedrock geology on knickpoint development and channel-bed degradation along downcutting streams in south-central Indiana. *The Journal of Geology, 99*(4), 591-605. https://doi.org/10.1086/629519

Mvondo Owono, F., Etoundi Akoa, P. R., & Ntsama Atangana, J. (2024). Post Pan-African landscape evolution in the Garoua-Gaschiga Region (North Cameroon, Central Africa): a record of neotectonic, volcanic and climatic controls. *Arabian Journal of Geosciences, 17*(3), 110. https://doi.org/10.1007/s12517-024-11873-z

Mvondo Owono, F., Ntamak-Nida, M. J., Dauteuil, O., Guillocheau, F., & Njom, B. (2016). Morphology and long-term landscape evolution of the South African plateau in South Namibia. *Cateneau, 142*, 47-65. https://doi.org/10.1016/j.catena.2016.02.012

Ndjigui, P-D., Yongué-Fouateu, R., Bilong, P., Bayiga, E. C., Oumarou, M. (2009). Geochemical survey of Pt, Pd and Au in the talcschists and the hornblendites, and in their weathered equivalents at Pouth-Kellé, Southern Cameroun. *Journal of the Cameroon Academy of sciences, 8*(2/3), 107-120.

Nédélec, A., Minyem, D., & Barbey, P. (1993). High-P—high-T anatexis of Archaean tonalitic grey gneisses: the Eseka migmatites, Cameroon. *Precambrian research, 62*(3), 191-205. https://doi.org/10.1016/0301-9268(93)90021-S

Ngako, V., Affaton, P., Nnangue, J. M., & Njanko, T. (2003). Pan-African tectonic evolution in central and southern Cameroon: transpression and transtensiondurinosinistral shear movements. *Journal of African Earth Sciences, 36*(3), 207-214. https://doi.org/10.1016/S0899-5362(03)00023-X

Njiké Ngaha, P. R. (1984). Contribution à l'étude géologique, stratigraphique et structurale de la bordure du bassin Atlantique au Cameroun. *Thèse Doctorat 3ème cycle, Faculté des Sciences de l'Université de Yaoundé*, 131.

Njonfang, E., Ngako, V., Moreau, C., Affaton, P., & Diot, H. (2008). Restraining bends in high temperature shear zones: the "Central Cameroon Shear Zone", Central Africa. *Journal of African Earth Sciences, 52*(1-2), 9-20. https://doi.org/10.1016/j.jafrearsci.2008.03.002

Nsangou Ngapna, M., Owona, S., Mvondo Owono, F., Balla Ateba, C., Manga Tsimi, V., Mvondo Ondoa, J., & Ekodeck ,G. E. (2020). Assessment of relative active tectonics in Edea - Eseka region (SW Cameroon, Central Africa). *Journal of African Earth Sciences, 164*, 103798. https://doi.org/10.1016/j.jafrearsci.2020.103798

Nsangou Ngapna, M., Owona, S., Youmen, D., Mpesse, J. E., Tckecke Mpote, F., Temfack, M., Ganwa, A. A., Mvondo Ondoa, J., Ratschbacher, L., & Ekodeck, G.E. (2013). Contrôle géologique des unitées morphotectoniques de la région d'Edéa-éséka (SW Cameroun). *Sciences de la Vie et de la Terre et Agronomie, 1*(1), 47-54.

Ntomba, S. M., Bisso, D., Magnekou Takamte, R. C., Ndong Bidzang, F., Messi Ottou, E. J., & Mvondo Ondoa, J. (2020). Crustal growth in the Mesoarchean plutonic belt from the Memve'ele area (Ntem Complex-southwestern Cameroon): Evidence of "early earth" transpressional tectonics. *Journal of Structural Geology, 141*, 104195. https://doi.org/10.1016/j.jsg.2020.104195

Ntomba, S.M., Ndong Bidzang, F., Messi Ottou, E.J., Goussi Ngalamo, J.F., Bisso D., Magnekou Takamte, R.C., & Mvondo Ondoa, J. (2016). Phlogopite compositions as an indicator of both the geodynamic context of granitoids and the metallogeny aspect in Memve'ele Archean area, northwestern Congo craton. *Journal of African Earth Sciences, 118*, 231-244. https://doi.org/10.1016/j.jafrearsci.2016.02.004

Owona, S. Mbola Ndzana, S. P., Mvondo Ondoa, J., Nsangou Ngapna, M., Nkabsaah, C., Ratschbacher, L., & Ekodeck, G. E. (2013a). Geological control of geomorphologic units in the Southwest (SW) Cameroon (Central Africa). *Journal of Geology and Mining Research, 4*(7), 152-167.

Owona, S., Mvondo Ondoa, J., & Ekodeck, G. E. (2013b). Evidence of quartz, feldspar and amphibole crystal plastic deformations in the Paleoproterozoic Nyong Complex shear zones under amphibolite to granulite conditions (West Central African Fold Belt, SW Cameroon). *Journal of Geography and Geology, 5*(3), 186-204. https://doi.org/10.5539/jgg.v5n3p186

Owona, S., Mvondo Ondoa, J., Ratschbacher, L., Mbola Ndzana, S. P., Tchoua, M. F., & Ekodeck, G. E. (2011). The geometry of the Archean, Paleo- and Neoproterozoic tectonics in the Southwest Cameroon. *Comptes Rendus Geosciences, 343*, 312-322. https://doi.org/10.1016/j.crte.2010.12.008

Owona, S., Mvondo Ondoa, J., Tichomirowa, M., Ratschbacher, L., Tchoua, M. F., & Ekodeck, G. E. (2012). New 207Pb/206Pb-Zr evaporation, metamorphic 87Rb/86Sr-WR-Bt ages and tectonic imprints in the Archean So'o Group (Ntem Complex/Congo Craton, SW Cameroon). *Global Journal of Geological Science, 10*(1), 99-109.

Pedrera, A., Pérez-Peña, J. V., Galindo-Zaldívar, J., Azañón, J. M., & Azor, A. (2009). Testing the sensitivity of geomorphic indices in areas of lowrate active folding (eastern Betic Cordillera, Spain). *Geomorphology, 105*(3), 218-231. https://doi.org/10.1016/j.geomorph.2008.09.026

Penaye, J., Toteu, S. F., Tchameni, R., Van Schmus, W. R., Tchakounté, J., Ganwa, A., Minyem, D., & Nsifa, E. N. (2004). The 2.1 Ga West central African belt in Cameroon: extension and evolution. *Journal of African Earth Sciences, 39*(3-5), 159-164. https://doi.org/10.1016/j.jafrearsci.2004.07.053

Pérez-Peña, J. V., Azañón, J. M., & Azor, A. (2009). CalHypso: An ArcGIS extension to calculate hypsometric curves and their statistical moments. Applications to drainage basin analysis in SE Spain. *Computers & Geosciences, 35*(6), 1214-1223. https://doi.org/10.1016/j.cageo.2008.06.006

Pérez-Peña, J. V., Azor, A., Azañón, J. M., & Keller, E. A. (2010). Active tectonics in the Sierra Nevada (Betic Cordillera, SE Spain): Insights from geomorphic indexes and drainage pattern analysis. *Geomorphology, 119*(1-2), 74-87. https://doi.org/10.1016/j.geomorph.2010.02.020

Pouclet, A., Tchameni, R., Mezger, K., Vidal, M., Nsifa, E., Shang, C., & Penaye, J. (2007). Archaean crustal accretion at the northern border of the Congo Craton (South Cameroon). The charnockite-TTG link. *Bulletin de la Société géologique de France, 178*(5), 331-342. https://doi.org/10.2113/gssgfbull.178.5.331

Ramírez-Herrera, M. T. (1998). Geomorphic assessment of active tectonics in the Acambay Graben, Mexican volcanic belt. *Earth Surface Processes and landforms: The journal of the british Geomorphological Group, 23*(4), 317-332. https://doi.org/10.1002/(SICI)1096-9837(199804)23:4%3C317::AID-ESP845%3E3.0.CO;2-V

Reed, J. C. (1981). Disequilibrium profile of the Potomac River near Washington, DC–A result of lowered base level or Quaternary tectonics along the Fall Line?. *Geology, 9*(10), 445-450. https://doi.org/10.1130/0091-7613(1981)9%3C445:DPOTPR%3E2.0.CO;2

Regnoult, J. M. (1983). Synthèse géologique du Cameroun: carte télé-interprétation des linéaments de la République Unie du Cameroun au Nord du 4ème parallèle, Direction des Mines et de la Géologie; Yaoundé.

Seeber, L., & Gornitz, V. (1983). River profiles along the Himalayan arc as indicators of active tectonics. *Tectonophysics, 92*(4), 335-367. https://doi.org/10.1016/0040-1951(83)90201-9

Segalen, P. (1967). *Les sols et la géomorphologie du Cameroun*. Office de la Recherche Scientifique et Technique Outre-Mer.

Seidl, M. A., & Dietrich, W. E. (1992). The problem of channel erosion into bedrock. *Catena, 23*, 101-124.

Selby, M. J. (1980). A rock mass strength classification for geomorphic purpose: with tests from Antarctica and New Zealand. *Zeitschrift für Geomorphologie, 24*(1), 31-51.

Shang, C. K., Satir, M., Siebel, W., Nsifa, N. E., Taubald, H., Liégeois, J. P., & Tchoua, F. M. (2004). Major and trace element geochemistry, Rb-Sr and Sm-Nd systematics of TTG magmatism in the Congo craton: case of the Sangmelima region, Ntem complex, southern Cameroon. *Journal of African Earth Science, 40*(1-2), 61-79. http://dx.doi.org/10.1016/j.jafrearsci.2004.07.005

Sharma, G., Champati ray, P. K., & Mohanty, S. (2018). Morphotectonic analysis and GNSS observations for assessment of relative tectonic activity in Alaknanda basin of Garhwal Himalaya, India. *Geomorphology, 301*, 108-120. https://doi.org/10.1016/j.geomorph.2017.11.002

Sheik Mohideen, A. R. (2021). Morphometric assessment of hydrogeomorphic processes and landscape evolution in the Kallar watershed (Western Ghats, India): regionalization and prioritization. *Arabian Journal Geosciences, 14*(18), 1-28. https://doi.org/10.1007/s.12517-021-08105-z

Shukla, D. P., Dubey, C. S., Ningreichon, A. S. Singh, R. P., Mishra, B. K., & Singh, S. K. (2014). GIS-based morpho-tectonic studies of Alaknanda river basin: a precursor for hazard zonation. *Nature Hazards, 71*, 1433-1452. https://doi.org/10.1007/s11069-013-0953-y

Siddiqui, S., & Soldati, M. (2014). Appraisal of active tectonics using DEM-based hypsometric integral and trend surface analysis in Emilia-Romagna Apennines, northern Italy. *Turkish Journal of Earth Sciences, 23*(3), 277-292. https://doi.org/10.3906/yer-1306-12

Sinha-Roy, S. (2002). Hypsométric and landform evolution: a case study in the Banas drainage basin, Rajasthan, with implications for Aravalli uplift. *Journal of Geological society of India, 60*, 7-26.

Strahler, A. N. (1952). Hypsometric (area-altitude) analysis of erosional topography. Geological society of America bulletin, 63(11), 1117-1142. https://doi.org/10.1130/0016-7606(1952)63[1117:HAAOET]2.0.CO;2

Taloor, A. K., Joshi, L. M., Kotlia, B. S., Alam, A., Kothyari, G. C., Kandregula, R. S., Singh, A.K., & Dumka, R. K. (2021). Tectonic imprints of landscape evolution in the Bhilangana and Mandakini basin, Garhwal Himalaya, India: a geospatial approach. *Quaternary International, 575*, 21-36. https://doi.org/10.1016/j.quaint.2020.07.021

Tchameni, R., Mezger, K., Nsifa, N. E., & Pouclet, A. (2000). Neoarchaean crustal evolution in the Congo Craton: evidence from K rich granitoids of the Ntem Complex, southern Cameroon. *Journal of African Earth Sciences, 30*(1), 133-147. https://doi.org/10.1016/S0899-5362(00)00012-9

Thakkar, M. G., Chauhan, G., Shah, Y., Jani, C., Chavada, B., Lakhote, A., Bhosale, S., & Mistry, C. P. (2021). Nepheline syenite and related rocks at Meruda Takkar hill, northern Kachchh: Neoproterozoic Malani

basement or Mesozoic alkaline magmatism?. *Journal of Earth System Science, 130*(1), 4. https://doi.org/10.1007/s12040-020-01493-y

Thierry, P., Stieltjes, L., Kouokam, E., Ngueya, P., Arnal, C., Gehl, P., & Salley M. P. (2006*). Projet GRINP – composante 1. Réalisation d'une carte de zonage des risques du Mont Cameroun*. Rapport final Rapport BRGM RC-54727-FR 3, 333.

Topal, S., Keller, E., Bufe, A., & Koçyiğit, A. (2016). Tectonic geomorphology of a large normal fault: Akşehir fault, SW Turkey. *Geomorphology, 259*, 55-69. https://doi.org/10.1016/j.geomorph.2016.01.014

Troiani, F., & Della Seta, M. (2008). The use of the Stream Length–Gradient index in morphotectonic analysis of small catchments: A case study from Central Italy. *Geomorphology, 102*(1), 159-168. https://doi.org/10.1016/j.geomorph.2007.06.020

Vicat, J. P., Nsifa, E., Tchameni, R., & Pouclet, A. (1998). La ceinture de roches vertes de Lolodorf-Ngomedzap (Sud-Cameroun). *Pétrologie, géochimie et cadre géodynamique. Géosciences au Cameroun, collect GEOCAM, 1*(1998), 325-337.

Vidal, M., Delor, C., Pouclet, A., Simeon, Y., & Alric, G. (1996). Evolution geodynamique de l'Afrique de l'Ouest entre 2, 2 Ga et 2 Ga; le style" archeen" des ceintures vertes et des ensembles sedimentaires birimiens du nord-est de la Cote-d'Ivoire. *Bulletin de la Société géologique de France, 167*(3), 307-319.

Wabo Defo, P. L., Owona, S., Nsangou Ngapna, M., Balla Ateba, C., & Mwabanua Mutabi, C. (2022). Post-orogenic transients and relict landforms of the Bafoussam-Mamfe region (West-Cameroon Highland margin). *Journal of Mountain Science, 19*(8), 2180-2201. https://doi.org/10.1007/s11629-021-7180-x

Willgoose, G., & Hancock, G. (1998). Revisiting the hypsometric curve as an indicator of form and process in transport-limited catchment. *Earth Surface Processes and Landforms: The Journal of the British Geomorphological Group, 23*(7), 611-623. https://doi.org/10.1002/(SICI)1096-9837(199807)23:7%3C611::AID-ESP872%3E3.0.CO;2-Y

Wobus, C., Whipple, K. X., Kirby, E., Snyder, N., Johnson, J., Spyropolou, K., Crosby, B. T., & Sheehan, D. (2006). *Tectonics from topography: procedures, promise, and pitfalls*. Geological Society of America Special Papers. http://doi.org/10.1130/2006.2398(04)

Xue, L., Gani, N., & Abdelsalam, M. G. (2017). Geomorphologic proxies for Bedrock Rivers: a case study from the Rwenzori Mountains, East African Rift System. *Geomorphology, 285*, 374-398. https://doi.org/10.1016/j.geomorph.2017.01.009